

1 of 1

AREST Model Description

**D. W. Engel
B. P. McGrail**

November 1993

**Prepared for
the U.S. Department of Energy
under Contract DE-AC06-76RLO 1830**

**Pacific Northwest Laboratory
Richland, Washington 99352**

MASTER

Executive Summary

The Office of Civilian Radioactive Waste Management (OCRWM) of the U.S. Department of Energy (DOE) and the Power Reactor and Nuclear Fuel Development Corporation of Japan (PNC) have supported the development of the Analytical Repository Source-Term (AREST) at Pacific Northwest Laboratory. The purpose of this report is to describe the mathematical models and logic of AREST.

AREST is a computer model developed to evaluate radionuclide release from an underground geologic repository. The AREST code can be used to calculate/estimate the amount and rate of each radionuclide that is released from the engineered barrier system (EBS) of the repository. The EBS is the man-made or disrupted area of the repository. AREST was designed as a "system-level" models to simulate the behavior of the total repository by combining "process-level" models for the release from an individual waste package or container. AREST contains primarily analytical models for calculating the release/transport of radionuclides to the host rock that surrounds each waste package. Analytical models were used because of the small computational overhead that allows all the input parameters to be derived from a statistical distribution. Recently, a one-dimensional numerical model was also incorporated into AREST, to allow for more detailed modeling of the transport process with arbitrary length decay chains.

The next step in modeling the EBS, is to develop a model that couples the probabilistic capabilities of AREST with a more detailed process model. This model will need to look at the reactive coupling of the processes that are involved with the release process. Such coupling would include: 1) the dissolution of the waste form, 2) the geochemical modeling of the groundwater, 3) the corrosion of the container overpacking, and 4) the backfill material, just to name a few. Several of these coupled processes are already incorporated in the current version of AREST.

Acknowledgments

The initial version of AREST was developed based on the analytical solutions developed by T. H. Pigford, P. L. Chambré, W.W.-L. Lee, and their students at the University of California at Berkeley. The current version still contains many of their solutions and thus we would like to acknowledge their fine work and thank them for sharing this work with us. We would also like to thank F. M. Ryan for his editorial review, and S. M. Johnson and C. L. Savard for formatting and publication assistance on this document. Finally, we would like to thank D. M. Elwood for his review of the document, especially of the analytical equations.

Contents

Executive Summary	iii
Acknowledgments	v
1.0 Introduction	1.1
2.0 Code Structure	2.1
3.0 Containment Modeling	3.1
4.0 Release Models	4.1
4.1 Wet-Continuous	4.1
4.1.1 Matrix Release	4.3
4.1.1.1 Solubility-Limited Diffusion Model	4.3
4.1.1.2 Solubility-Limited Diffusion/Advection Model	4.4
4.1.1.3 Solubility-Limited Fracture Model	4.5
4.1.1.4 Reaction-Rate Limited Diffusion Model	4.7
4.1.1.5 Numerical-Transport Model	4.9
4.1.2 Gap Release	4.9
4.1.3 Cladding Release	4.10
4.2 Wet-Drip	4.11
4.2.1 Matrix Release	4.11
4.2.1.1 Solubility-Limited Advection Model	4.11
4.2.1.2 Reaction-Rate Limited Advection Model	4.12
4.2.2 Gap Release	4.13
4.2.3 Cladding Release	4.14
5.0 Waste-Form Surface Boundary Conditions	5.1

5.1	Input Values	5.1
5.2	Glass Dissolution Model	5.1
6.0	Radionuclide Inventory Models	6.1
6.1	Exhaustion Model	6.1
6.2	Decay Chain Models	6.1
6.2.1	Long-Lived Parent/Very Short-Lived Daughter	6.2
6.2.2	Long-Lived Parent/Short-Lived Daughter	6.2
6.2.3	Short-Lived Parent/Long-Lived Daughter	6.3
7.0	Support Codes	7.1
7.1	Thermal Modeling	7.1
7.2	Geochemical Modeling	7.1
7.3	Radiological Modeling	7.2
7.4	Hydrological Modeling	7.2
8.0	AREST Code Future	8.1
9.0	References	9.1
	Appendix A - Release Model Verification	A.1
	Appendix B - Geochemical Data Input for Glass Model	B.1
	Appendix C - Input And Support Code Data Files	C.1

Figures

2.1	AREST System Structure	2.2
4.1	Possible Release Modes of AREST ("Wet-Continuous")	4.2
4.2	Possible Release Modes of AREST ("Wet-Drip")	4.2
A.1	Verification Plot for the PDS Matrix Release Model (UCBMAT)	A.3
A.2	Verification Plot for the PCS Matrix Release Model (UCBCONV)	A.3
A.3	Verification Plot for the Fissure/Fracture Matrix Release Model (UCBFISS)	A.4
A.4	Verification Plot for the PDR Matrix Release Model (UCBALT)	A.4
A.5	Verification Plot for the Numerical Release Model (STRENG)	A.5
A.6	Verification Plot for the Inventory-Limited/GAP Release Model (UCBGAP)	A.5
A.7	Verification Plot for the Solubility-Limited Release Model for "Wet-Drip"	A.6
A.8	Verification Plot for the Alteration-Limited Release Model "Wet-Drip"	A.6
A.9	Verification Plot for the Inventory-Limited/GAP Release Model for "Wet-Drip"	A.7
A.10	Base Case for Comparing with Glass Dissolution Model	A.7
A.11	Plot for the Glass Dissolution Model Not Considering Iron Corrosion	A.8
A.12	Plot for the Glass Dissolution Model Considering Iron Corrosion	A.8
B.1	Effect of Iron on the Reaction Affinity of P0798 Glass	B.8

Tables

A.1	AREST Input Data File for the Verification of the Diffusive/Advective Release Model (PCS)	A.9
B.1	Example Input File for EQ3NR	B.4
B.2	Example Input File for the EQ6 Code	B.6
C.1	Sample Input Data File for AREST	C.4
C.2	Example of a Repository Average Temperature Distribution File	C.11
C.3	Example of a Reference Container Temperature Distribution File	C.12
C.4	Sample Cumulative Probability Distribution for Heat Loading	C.13
C.5	Sample Groundwater Composition Data File	C.13
C.6	Sample Temperature Dependent Solubility Data File	C.14
C.7	Sample File When NOT Modeling Temperature Dependent Solubilities	C.14
C.8	Sample Concentration Data File Used With the Glass Dissolution Model	C.15
C.9	Sample Affinity Data File Used With the Glass Dissolution Model	C.16

1.0 Introduction

The Office of Civilian Radioactive Waste Management (OCRWM) of the U.S. Department of Energy (DOE) is investigating the permanent disposal of radioactive waste in an underground geologic repository. OCRWM has supported the Performance Assessment Scientific Support (PASS) program at Pacific Northwest Laboratory (PNL),^(a) to develop a source-term model for evaluating radionuclide release from an engineered barrier system (EBS) of an underground geological repository. The Analytical Repository Source-Term (AREST) computer code was developed for this analysis (Liebetrau et al. 1987; Engel et al. 1989). The AREST code development supported by DOE, consists of the following features:

- analytical models for the release/mass transfer of nuclides through a backfill region and into a surrounding host rock
- a limited number of input parameters that could be modeled using a statistical distribution (stochastic)
- a simple spent fuel dissolution model for estimating the concentration of each nuclide at the waste form surface
- radionuclide decay in the waste form and in the release models, but no consideration of decay-chain ingrowth during transport
- analysis done using batch mode (no user-interface) with input and output through data files.

The Power Reactor and Nuclear Fuel Development Corporation of Japan (PNC) subsequently funded PNL to enhance the AREST code (Engel et al. 1992; Nakamura and Wilkins 1992). The enhancements included the following:

- implementing a numerical transport model
- developing a graphical user-interface that allowed the input of all parameters interactively using a windowing environment and allowing all input parameters to be stochastic or be modeled as a range of values
- developing and implementing a glass dissolution model that coupled the reaction of the glass, the groundwater, an iron overpack/container, and a clay backfill
- implementing decay chain models for estimating the effect of ingrowth during transport to the surrounding host rock

(a) Pacific Northwest Laboratory is a multiprogram national laboratory operated for the U.S. Department of Energy by Battelle Memorial Institute under contract DE-AC06-76RLO 1830.

- developing a graphical user-interface to make the AREST code interactive, easy to input and modify parameters, and graphically display the results.

The AREST code contains three different modules/routines. The first module is the input manager, which allows the user to input data and set up the analysis. The second module is the AREST model. This contains the computational models for calculating the release from the EBS. Finally, there is the plot manager, which allows the user to graphically display the results. The purpose of this document is to describe the AREST model and the computational capabilities of the code. The user interface, input manager, and plot manager are described elsewhere (Nakamura and Wilkins 1992). The term AREST will be used in this document to mean the modeling part of the AREST code (AREST model).

This document has nine sections and three appendices. Section 2.0 describes the structure and logic of AREST. The containment modeling is then discussed in Section 3.0.

Section 4.0 contains a mathematical description of the release models that are contained in AREST. Calculating the concentrations of a radionuclide, at the waste form boundary, is discussed in Section 5.0. AREST contains the capability to either input a surface concentration as a single value or as a time-dependent value (Section 5.1). AREST can also use a glass dissolution model for estimating the surface concentration. The glass dissolution model is described in Section 5.2.

Section 6.0 describes the radionuclide inventory models that are contained in AREST. Section 6.1 discusses the exhaustion model used for the depletion of a nuclide in the waste form. The decay chain model for estimating the ingrowth of a nuclide during transport is described in Section 6.2.

AREST utilizes detailed analyses done outside the code for physical, chemical, and nuclear processes. The results of the analyses are then input to AREST through lookup tables and response functions. This detailed analyses, called support code modeling, is discussed in Section 7.0. Section 7.1 describes the thermal modeling that is done for AREST. The geochemical modeling used by AREST is discussed in Section 7.2, while the radiological/inventory modeling is discussed in Section 7.3. Finally, the hydrological modeling for saturation and groundwater flow is discussed in Section 7.4.

Section 8.0 contains a brief description of the planned development of the AREST code. The version of AREST that is discussed in this document can be used to get an overall quantitative systems-level estimate for the release from the EBS, including simple sensitivity and uncertainty analysis. This version, however, lacks capabilities for modeling several processes that are expected to be important at the candidate repository site. Thus a more detailed model, using numerical methods is needed for a better estimate of the performance of the EBS.

Three appendices are included in this document. Appendix A shows a verification of the release models that are incorporated in AREST. Appendix B discusses the geochemical modeling that is needed for the glass dissolution model. Appendix C contains a listing and description of the input data file and input support code data files that are read by AREST.

2.0 Code Structure

AREST was developed as a "system-level" model, as opposed to a "process-level" model. This means that AREST calculates the release from the overall system as opposed to the effect that each process has on the release. AREST was developed to provide a quantitative probabilistic assessment of the performance of the individual barriers of the overall EBS. In AREST, the waste package has been established as the basic unit of simulation. The waste package consists of the waste container, a backfill region of some type of porous media (e.g., bentonite or crushed tuff) or an air gap surrounding the container, and a host rock surrounding the backfill/air gap region.

The structure of the total AREST system is shown in Figure 2.1. The AREST system consists of: 1) external analysis describing the physical and chemical environment of the repository and waste package (support code analysis), 2) external input process that allows for sensitivity and uncertainty analyses (input manager), 3) the computational models that make up the AREST code, and 4) external plot routines that graphically display the results from the AREST code (plot manager). In Figure 2.1, the processes external to the AREST code (support codes, input manager, and plot manager) are shown by dashed boxes, while the computational models that make up the AREST model are shown with solid boxes. Most of the material in this document describes the computational part of the AREST system. For the remainder of this document, the term AREST will be used when discussing the AREST model, or the computational part of the AREST system.

The first step in AREST, as shown in Figure 2.1, is input. Input into AREST is done through data files. A sample input file is shown and described in Appendix C. After the input step, AREST simulates a temperature profile over the lifetime of the waste package. A different temperature profile is simulated for each waste package. The actual simulation of temperature profiles in AREST has been described in detail elsewhere (Liebetrau et al. 1987) and is also briefly described in Section 7.1 of this document.

Next, the temperature dependent groundwater composition, as calculated by support code analysis, is read into AREST. The process for the groundwater modeling of AREST is described in detail by Liebetrau (Liebetrau et al. 1987) and is briefly described in Section 7.2.

With a temperature profile and a groundwater composition, containment is then simulated. Logic has been incorporated in AREST to simulate uniform corrosion, pitting corrosion, and stress corrosion cracking of the container with a user-defined model of the corrosion process. Containment can also be modeled using statistical distributions. The modeling of containment in AREST is described in further detail in Section 3.0.

After loss of the containment barrier has been simulated, radionuclide inventories are calculated. Inventories at time of emplacement, as calculated by the external radiological support codes (described in Section 7.3), are input directly into AREST. Time dependent inventories after the time of containment failure are calculated using the Bateman equations (Benedict and Pigford 1957).

The last step in the computational process of AREST is to calculate, for each nuclide, the release and transport to the surrounding host rock. This process consists of: 1) dissolution of the

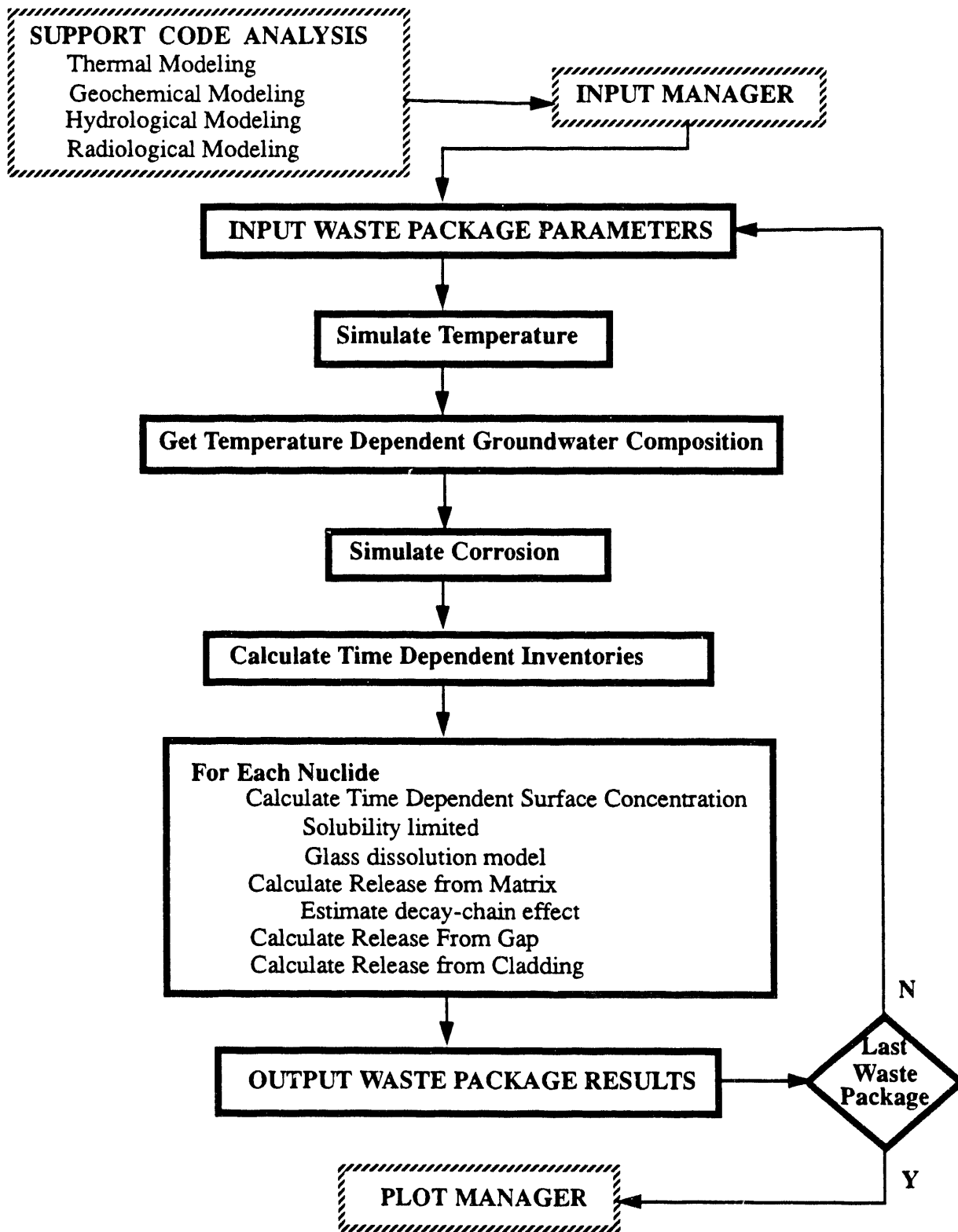


Figure 2.1. AREST System Structure. Solid boxes are contained in the AREST model.

radionuclide from the waste form (Section 5.0), 2) transport through a backfill or an air gap surrounding the waste container (Section 4.0), 3) transport into the host rock (Section 4.0), and 4) the effect of decay chain ingrowth for release from the matrix of the waste form (Section 6.2).

The results for the simulated waste package, release rates or concentrations at the boundary of the backfill and the surrounding host rock, are then output to a data file. If this was the last waste package to be simulated, the program terminates; otherwise, the logic transfers back to the input routine to simulate another waste package.

3.0 Containment Modeling

The current philosophy for modeling containment in AREST is to model the effective life of a waste container by a realization from a statistical distribution, where a penetration of the container is assumed at some time after emplacement into the repository. Statistical models are used to simulate containment failure times because of the lack of defensible corrosion models for the container designs being considered by the Yucca Mountain Project.

Currently, there are several statistical distributions in AREST, from which the user can select to simulate the time of containment failure for each waste package. The current distributions with the needed input parameters and the unit of time in years are as follows:

- point/degenerate distribution (single failure time for all waste packages)
- normal distribution, truncated so that $t_{\text{failure}} > 0.0$ (mean failure time, standard deviation)
- uniform distribution (minimum failure time, maximum failure time)
- exponential distribution (minimum failure time, decay constant)
- symmetrical triangle distribution (minimum failure time, maximum failure time).

Logic exists in AREST to model different corrosion process, including uniform corrosion of the container/overpack. Containment is assumed to be lost when the overpack has lost the ability to withstand lithostatic load due to uniform corrosion. There also exists logic to model pitting and stress corrosion cracking of the overpack coupled with uniform corrosion of the cladding, when spent fuel is being modeled. The corrosion model compares the different types of failure modes (uniform corrosion of the overpack, pitting of the overpack with uniform corrosion of cladding, and stress corrosion cracking of the overpack with uniform corrosion of cladding) and selects the appropriate failure mode.

Once containment has been lost, any mass transport resistance that may exist due to partial failure of the overpack is neglected. This is a conservative assumption that is implemented in AREST because of the extraordinary difficulty in quantifying the geometry and number of cracks or pinhole failures far into the future.

4.0 Release Models

For each simulated waste package, AREST estimates the release from the EBS at the interface between the backfill surrounding the waste container, or an air gap, and the surrounding host rock. The main measure of performance for the EBS, as calculated in AREST, is the release rate.

AREST has been designed so that the user can specify the mode of release, the water contact mode, and a specific release model. AREST uses a single release model for a specific release and water contact mode. The possible release modes are shown in Figures 4.1 and 4.2. The modes of release in the AREST code are defined by the following conditions:

- groundwater flow: pore flow versus fracture flow
- transport: diffusive versus diffusive-convective transport into the host rock
- controlling concentration at the waste form surface: reaction-rate limited versus solubility-limited.

AREST also considers two types of water contact mode, "wet-continuous" or "wet-drip". The modes of release, water contact modes, and the release models implemented in AREST are shown in Figures 4.1 and 4.2, shaded boxes, and are discussed in the following sections. The equations that are presented in this document represent the final form of the equation, as implemented in AREST. A reader who is interested in more details about the models, e.g., governing equations or more detailed assumptions, should refer to the referenced material.

4.1 Wet-Continuous

This type of water contact mode assumes that a continuous diffusive pathway exists from the waste form surface to the host rock. For the designs being considered at Yucca Mountain, this diffusive pathway may exist due to a backfilled region between the waste container and the host rock, in a robust design, by contact of the waste container and the host rock due to physical displacement of the waste container, or by sedimentation of rubble, crushed tuff, in the air gap that may surround the waste container. For the remainder of this document, we use the term "backfill" to mean any diffusive pathway between the waste container and the host rock, such as a clay or crushed tuff backfill or a rubble-filled region.

AREST can model three different sources for radionuclide release: matrix, gap, and spent fuel cladding. Each of these three sources is modeled separately with the distribution for each source being specified by the user (e.g., ^{14}C : 65 percent in matrix, 2 percent in gap, and 33 percent in cladding). The models for each source for the wet-continuous water contact mode are described in the following sections.

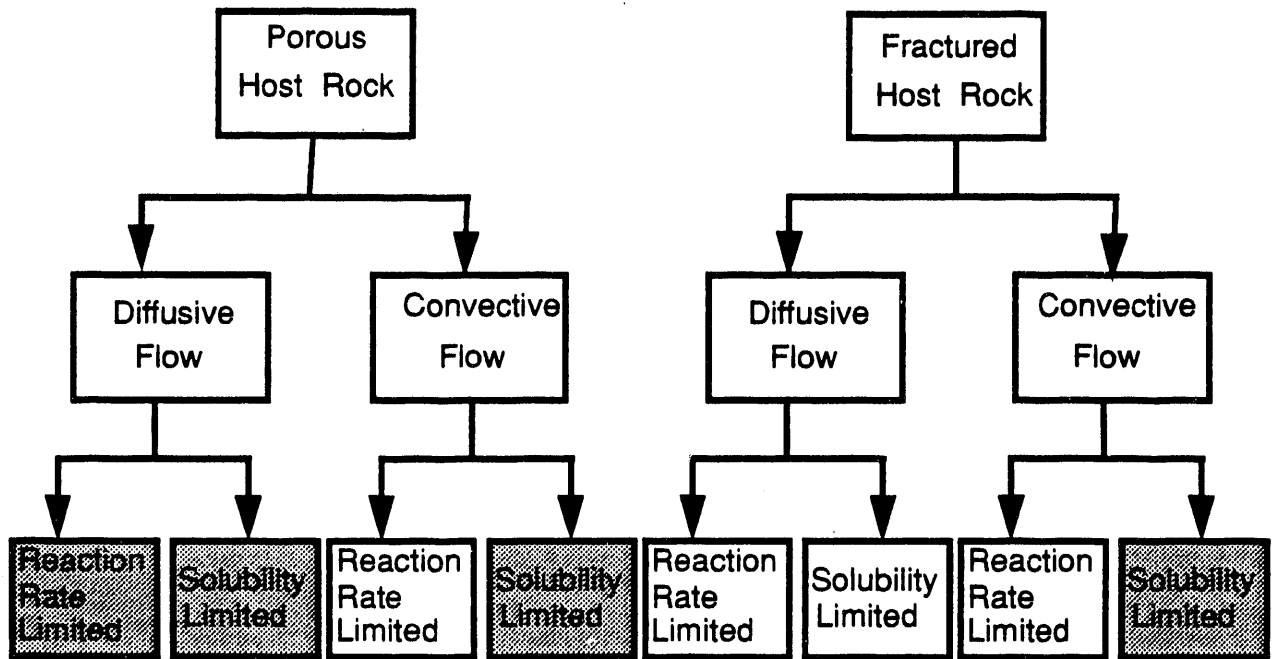


Figure 4.1. Possible Release Modes of AREST. Shaded boxes imply models that currently exist in AREST for a "wet-continuous" water contact mode.

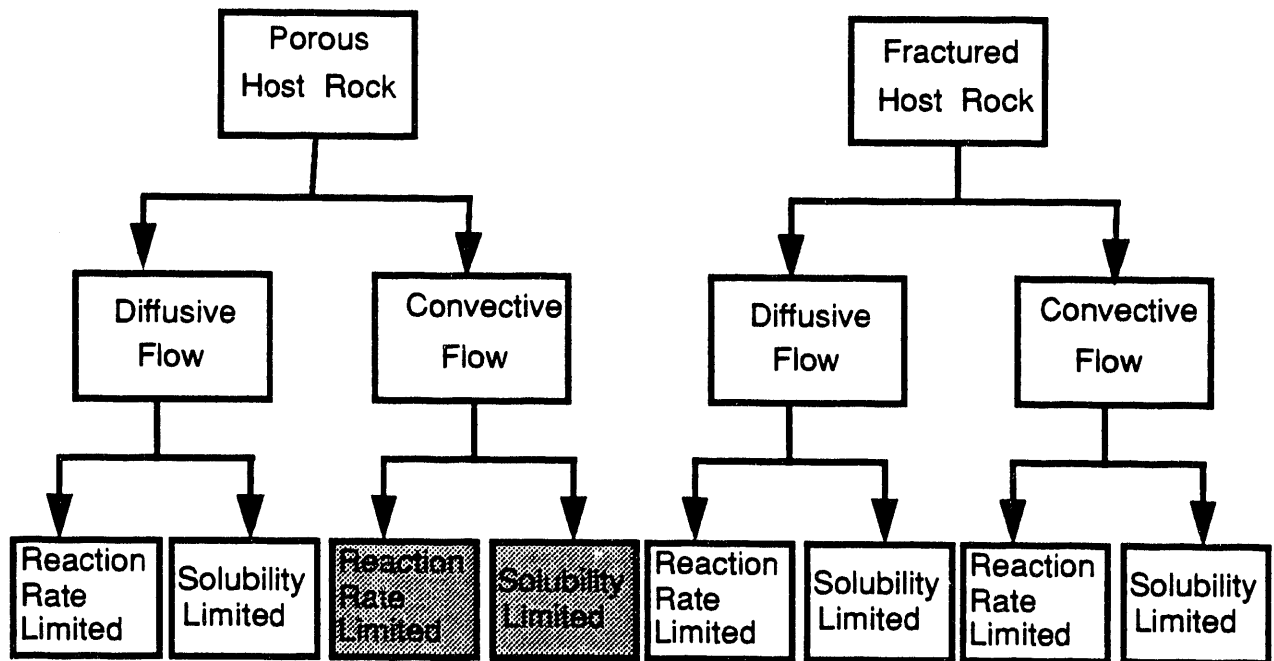


Figure 4.2. Possible Release Modes of AREST. Shaded boxes imply models that currently exist in AREST for a "wet-drip" water contact mode.

4.1.1 Matrix Release

For spent UO_2 fuel, more than 99 percent of the radionuclides are contained within the UO_2 matrix grains (Liebetrau et al. 1987). It is assumed that all of the models for the matrix release are valid for both spent fuel and glass waste forms. AREST assumes that each element is released congruently with the dissolution of the waste matrix (reaction-rate limited), or else the solution concentration at the surface of the waste form is calculated by a solubility limit (solubility-limited). Transport from the waste form to the host rock is assumed to be dominated by either diffusion or by diffusion/advection in the backfill zone. Finally, transport into the host rock is either by diffusion into the rock matrix or by advection into fractures in the rock. The shaded boxes in Figure 4.1 show the modes of release where models currently exist in AREST. These models are described below.

4.1.1.1 Solubility-Limited Diffusion Model

An analytical model developed at the University of California at Berkeley (UCB) for estimating release based on diffusive mass transport through a backfill and into a porous host rock has been implemented into AREST (Pigford et al. 1990). The model assumes a solubility-limited constant concentration at the waste form surface and a waste package that is modeled as a sphere. Transport occurs through a backfill and into a semi-infinite porous host rock surrounding the waste package. The release rate from spent fuel or a glass waste form (\dot{M}_i , g/yr) as a function of the distance in the backfill (r , cm) and time (t , yrs) is calculated as follows:

$$\dot{M}_i(r,t) = 4\pi\sigma_1\epsilon_1 D_f R_0 r C_i^S \psi_i(r,t) \quad (1)$$

where C_i^S (g/m^3) is the surface concentration for nuclide i , ϵ_1 and ϵ_2 are the porosities of the backfill and host rock, respectively, σ_1 and σ_2 are the tortuosities of the backfill and host rock, respectively, D_f (cm^2/s) is the diffusion coefficient for nuclide i in water, R_0 and R_1 (cm) are the waste form radius and the waste package radius, respectively, and ψ_i is a function defined as:

$$\psi_i(r,t) = \frac{1}{r\left(1 + \gamma \frac{R_0}{R_1}\right)} - \int_0^{\infty} (I_1(\eta)I_2(\eta))d\eta, \quad R_0 \leq r \leq R_1, \quad 0 < t \quad (2)$$

where

$$I_1(\eta) = \frac{1}{1 + \frac{D_1\eta^2}{\lambda}} + \frac{e^{(-D_1\eta^2 - \lambda t)}}{1 + \frac{\lambda}{D_1\eta^2}} \quad (3)$$

$$I_2(\eta) = \frac{2\sigma_1\epsilon_1\sigma_2\epsilon_2\beta}{\pi} \frac{\eta \left(\cos(\eta[r - R_0]) \frac{1}{r} \sin(\eta[r - R_0]) \right)}{[\sigma_1\epsilon_1\eta\cos(\eta b) + \alpha\sin(\eta b)]^2 + [\beta\sigma_2\epsilon_2\eta\sin(\eta b)]^2} \quad (4)$$

$$D_1 = \frac{D_f}{K_1} \quad (5)$$

$$\alpha = \frac{\sigma_1\epsilon_1 - \sigma_2\epsilon_2}{R_1} \quad (6)$$

$$\beta = \sqrt{\frac{K_1}{K_2}} \quad (7)$$

$$\gamma = \frac{\sigma_1\epsilon_1 - \sigma_2\epsilon_2}{\sigma_2\epsilon_2} \quad (8)$$

where K_1 and K_2 are the retardation coefficients in the backfill and host rock respectively, λ is the radioactive decay constant (yr^{-1}), and b is the backfill thickness ($R_1 - R_0$, cm). The retardation coefficient in either the backfill or the host rock is calculated from the sorption coefficient (K_d , ml/g), the bulk density (ρ_b , g/m^3), and the porosity (ϵ) as:

$$K_l = 1 + \frac{\rho_b K_d}{\epsilon_l} \quad l = 1, 2 \quad (9)$$

4.1.1.2 Solubility-Limited Diffusion/Advection Model

In the previous section, radionuclide release into the host rock was assumed to occur by diffusion. Another possible scenario for some host rocks is that advection is the dominant transport process. A steady-state mass transport model has been developed (Pigford et al. 1990) and implemented into AREST to analyze this scenario. The model is applicable to the steady-state mass transport of a radioactive species assuming the waste container is a sphere with a backfill surrounded by a porous host rock. The model assumes a solubility-limited boundary condition at the waste form with diffusive transport through the backfill and diffusive/advective transport into the host rock. The equations for the steady-state release rate (\dot{M} , g/yr) are listed as follows:

$$\dot{M}_i(R_1) = \frac{4\pi\sigma_1\epsilon_1 D_f R_0 C_i^S (Sh \cdot R_1 \sqrt{K})}{(Sh - 1)\sinh(d) + R_1 \sqrt{K} \cosh(d)} \quad (10)$$

where

$$K = \frac{\lambda \frac{K_1}{\sigma_1}}{D_f} \quad (11)$$

$$d = (R_1 - R_0)\sqrt{K} \quad (12)$$

$$Sh = 1 + \frac{0.5Pe}{1 + 0.63\sqrt{Pe}} \quad (13)$$

$$Pe = \frac{R_1 U}{D_f} \quad (14)$$

where ϵ_1 , D_f , R_0 , R_1 , λ , K_1 , and C_i^S are as defined before, Sh is the calculated Sherwood number, Pe is the calculated Peclet number, and U (m/yr) is the groundwater pore velocity. The model was developed for Peclet numbers greater than 1.0, but will work for all values of Pe . For Peclet numbers much less than 1.0 ($Pe \ll 1.0$), the model is relatively unaffected by the pore velocity, U .

4.1.1.3 Solubility-Limited Fracture Model

Fractures or fissures in the host rock may intersect nuclear waste packages in some geologic formations. If there is convective flow in the fractures, this will provide conductive pathways for the transport of radionuclides from the near-field to the far-field and beyond. Because the water flowing in the fissure provides the main hydrologic pathway for radionuclide transport in the far-field, it may be conservatively assumed that the low porosity matrix of the fractured rock surrounding the backfill is impervious to transport, at least compared to transport in the fracture. Therefore, release from the waste package is assumed to be dominated by diffusional transport through the backfill and diffusion/advection into fractures where water is flowing.

Researchers at UCB (Kang 1990; Pigford et al. 1990) have developed a general, time-dependent model for this fracture scenario. A fixed solubility-limited concentration for each radionuclide is assumed at the surface of the waste form. The boundary condition at the backfill-fracture interface is given by a mass balance of the diffusional flux of each nuclide through the backfill with convective transport into the fracture. The flux is normalized by the cross-sectional area where the fracture intersects the waste package. The cylindrical geometry of the waste package is approximated by a rectangular parallelepiped, resulting in a simplified two-dimensional rectangular geometry. The analysis is further simplified by replacing the complex spatial dependence of concentrations for each

nuclide at the fracture opening with an average concentration, $[c(T)]_{av}$. This term is a complex function of previously defined parameters λ , b , K_1 , D_f , ϵ_1 , as well as the thickness of the fracture aperture (a , cm), and the length of the waste package (l , cm). The equations for the average concentration, $[c(T)]_{av}$, are:

$$[c(T)]_{av} = f(T) + \int_0^T K(T, \tau) [c(\tau)]_{av} d\tau \quad (15)$$

where

$$f(t) = \frac{1}{\cosh \Lambda} + 2 \sum_{i=0}^{\infty} (-1)^{i+1} \frac{\tilde{\gamma}_i}{\tilde{\gamma}_i^2 + \Lambda^2} e^{-(\tilde{\gamma}_i^2 + \Lambda^2)T} \quad (16)$$

$$K(T, \tau) = -2Sh \sum_{n=0}^{\infty} \delta_n \frac{\sin^2\left(\tilde{\mu}_n \frac{a}{l}\right)}{\tilde{\mu}_n^2 \frac{a}{l}} \sum_{i=0}^{\infty} e^{-(\tilde{\gamma}_i^2 + \tilde{\mu}_n^2 \frac{a}{l} + \Lambda^2)(T-\tau)} \quad (17)$$

$$\mu_j = \frac{j\pi}{l}, \quad \hat{\gamma}_j = \frac{2j+1}{2} \cdot \frac{\pi}{b}, \quad j = 0, 1, 2, \dots \quad (18)$$

$$\tilde{\gamma}_i = \hat{\gamma}_i b, \quad \tilde{\mu}_n = \mu_n l \quad (19)$$

$$T = \frac{D_f t}{K_1 b^2}, \quad \text{Modified Fourier modulus} \quad (20)$$

$$Sh = \frac{H b}{D_f \epsilon_1}, \quad \text{Modified Sherwood modulus} \quad (21)$$

$$\Lambda = \sqrt{\lambda b^2 \frac{K_1}{D_f}}, \quad \text{Modified Thiele modulus} \quad (22)$$

where H (m^3/yr) is the mass transfer coefficient at the backfill/fracture interface and is calculated using the following equation (Hwang and Pigford 1990):

$$H = 4a \sqrt{U \epsilon R_1 \frac{D_f}{\pi}} + 2\pi \epsilon_1 D_f \frac{h - \frac{a}{2}}{\ln\left(\frac{R_1}{R_2}\right) \cdot \ln\left(\frac{2h}{a}\right)} \quad (23)$$

where U (g/m^3) is the pore water velocity in the fracture, ϵ is the porosity in the fracture, and h (cm) is the fracture spacing. The resultant H value must be divided by the total surface area of the fracture that intersects the waste package to obtain units of "m/yr".

The final equation for calculating the time-dependent, mass transfer rate (\dot{M} , g/yr) into a fracture is (Kang 1990):

$$\dot{M}_i(R_1, t) = 2\pi C_i^s \epsilon_1 \sigma_1 D_f R_1 S h \frac{a}{b} [c(T)]_{av} \quad (24)$$

where the terms are as defined previously for the other release models. The mass transfer coefficient presented earlier is used for all ranges of parameters. The most relevant range for the use of this form of the mass transfer coefficient is with a Peclet number greater than 4. It is advised, therefore, that the user be aware of the Peclet number and the relevance of the equations.

4.1.1.4 Reaction-Rate Limited Diffusion Model

The mass transfer rate for highly soluble nuclides may be limited by the rate of reaction of the waste form instead of a solubility limit, as was assumed in the previous models. We have implemented a model to treat this reaction-rate limited case. In this model, groundwater flow is assumed to be small enough that the mass transfer through the backfill and into the semi-infinite porous host rock is controlled by molecular diffusion. The model also assumes that the waste starts to dissolve as soon as the container fails.

An approximate solution for this scenario was developed based on a model for the gap/grain boundary release (Section 4.1.2 of this document and Kang 1990). The total dissolution time (t_{diss} , yrs) it takes to dissolve the entire waste form of mass M^0 (g), is divided into a certain number of equal time intervals ($ndp = 100$ in the current version). For each time interval of the dissolution period, j , it is assumed that an equal amount of waste (M_j^0 , g) is dissolved. It is also assumed that the mass for each time interval dissolves instantaneously at the beginning of each time interval (e.g., $ndp = 100$, $M^0 = 1000$ g $\rightarrow M_j^0 = 10$ g/interval). It is further assumed that the amount dissolved during each time interval is transported through the backfill and into the host rock using the following equations for the release rate ($\dot{M}_{i,j}$, g/r):

$$\dot{M}_{i,j}(R_1, t_j) = 2K_1 \epsilon_1 \psi_1 N^0 S \frac{e^{-\lambda t_j}}{\delta + 1} \sum_{n=0}^{\infty} \left[\left(\sqrt{\frac{D_1}{\pi t_j}} - \Omega_0 D_1 H(\phi_n^2) \right) e^{\left(\frac{(2n+1)^2 b^2}{4D_1 t_j} \right)} \right] \left[\frac{\delta - 1}{\delta + 1} \right]^n \quad (25)$$

$$H(z^2) = e^{-z^2} \operatorname{erfc}(z) \quad (26)$$

$$\phi_n = \frac{(2n + 1)b}{2\sqrt{D_1 t}} + \Omega_0 \sqrt{D_1 t} \quad (27)$$

$$D_1 = \frac{D_f \sigma_1}{K_1} \quad (28)$$

$$\delta = \frac{\epsilon_1 \psi_1 \sqrt{\frac{K_1 \sigma_1}{K_2 \sigma_2}}}{\epsilon_2 \psi_2} \quad (29)$$

$$\Omega_0 = K_1 \epsilon_1 \psi_1 \frac{S}{V} \quad (30)$$

where ψ_1 and ψ_2 are the saturation fractions in the backfill and host rock, respectively, S (cm²) is the surface area at the waste-backfill interface which is assumed to be equal to the surface area of the waste cylinder, V (cm³) is the volume of all the void in the container and is equal to the difference in the volumes of the cylindrical waste container and the total volume of the enclosed waste, and N^0 (g/m³) is the concentration in the gap/void and is calculated by dividing the mass of the nuclide in the gap/void (for each time interval) by the volume of the gap/void ($N^0 = M_j^0/V$).

The total release rate into the host rock for nuclide i over time is then derived by summing the series of $\dot{M}_{i,j}$ terms, each offset for the time interval, given by:

$$\dot{M}_i(R_1, t) = \sum_{j=1}^{ndp} \dot{M}_{i,j}(R_1, t'_j) \quad (31)$$

where

$$t'_j = t - (j - 1) \frac{t_{dis}}{ndp - 1} \quad (32)$$

Linear interpolation is used to get release rates for each ndp series for the t'_j time steps. This summation is continued until the waste form is completely dissolved or until the inventory of each nuclide is exhausted in the waste form due to radioactive decay.

4.1.1.5 Numerical-Transport Model

AREST contains primarily analytical models for estimating radionuclide release rates. A natural extension to the capabilities of AREST has been to implement a numerical release model. The numerical model STRENG (Grindrod et al. 1991) was selected for the current version of AREST. STRENG was originally developed for the Swiss National Cooperative for the Disposal of Radioactive Waste (NAGRA) by the Environmental Division of Intera Technologies (formerly Intera Sciences).

STRENG is a one-dimensional finite difference model that analyzes the diffusive release of radionuclides assuming cylindrical geometry. The model includes the dissolution of the waste matrix together with the effects of: 1) solubility limits, 2) diffusive transport through a backfill, and 3) radionuclide decay and ingrowth. The user has the option to use either a zero concentration at the host rock boundary (swept away condition, semi-infinite host rock) or a "mixing tank" condition (finite length host rock).

4.1.2 Gap Release

During operation of a nuclear reactor, fission products can accumulate in the gaps and grain boundaries of the fuel rods. These highly soluble species, such as cesium and iodine, are expected to dissolve rapidly when groundwater enters the container. A model for approximating the release was developed at UCB (Kang 1990). The model includes diffusion of soluble species through a backfill into a surrounding rock in one-dimensional planar geometry.

It is assumed that over the time scale of interest, groundwater immediately fills a void volume (gap). A certain mass of nuclide is assumed to dissolve instantaneously from the waste form into this void, providing an initial concentration. The equations for the mass transfer rate, \dot{M} (g/yr), of highly soluble nuclides into the host rock are:

$$\dot{M}_i(R_1, t) = 2K_1 \epsilon_1 \psi_1 N^0 S \frac{e^{-\lambda t}}{\delta + 1} \sum_{n=0}^{\infty} \left[\left(\sqrt{\frac{D_1}{\pi t}} - \Omega_0 D_1 H(\phi_n^2) \right) e^{-\frac{(2n+1)^2 b^2}{4D_1 t}} \right] \left[\frac{\delta - 1}{\delta + 1} \right]^n \quad (33)$$

$$H(z^2) = e^{-z^2} \operatorname{erfc}(z) \quad (34)$$

$$\phi_n = \frac{(2n + 1)b}{2\sqrt{D_1 t}} + \Omega_0 \sqrt{D_1 t} \quad (35)$$

$$D_1 = \frac{D_f \sigma_1}{K_1} \quad (36)$$

$$\delta = \frac{\epsilon_1 \psi_1}{\epsilon_2 \psi_2} \sqrt{\frac{K_1 \sigma_1}{K_2 \sigma_2}} \quad (37)$$

$$\Omega_0 = K_1 \epsilon_1 \psi_1 \frac{S}{V} \quad (38)$$

where ψ_1 and ψ_2 are the saturation fractions in the backfill and host rock, respectively, S (cm²) is the surface area at the waste-backfill interface which is assumed to be equal to the surface area of the waste cylinder, V (cm³) is the volume of all the void in the container and is equal to the difference in the volumes of the cylindrical waste container and the total volume of the enclosed waste, and N^0 (g/m³) is the concentration in the gap/void and is calculated by dividing the mass of the soluble nuclide in the gap/void by the volume of the gap/void. It should be noted that this model is only applicable for modeling release through a backfill region. If no backfill exists ($b = 0$), then the model depends only on the backfill properties and not the host rock, even though no backfill exists.

4.1.3 Cladding Release

Another source of radionuclide release in spent fuel is the zircaloy cladding that surrounds the fuel rods. AREST includes the capability to model the cladding using two sources of release, clad and crud. The crud pertains to the part of the cladding that is readily accessible for release as soon as the overpack is breached. The clad pertains to the part of the cladding that is contained in the matrix of the cladding and releases as the cladding dissolves.

Modeling the release of the crud part of the cladding release is identical to the modeling done for the gap release. It is assumed that over the time scale of interest that a certain mass of nuclide (¹⁴C) is dissolved instantaneously from the cladding into the void. The equations for the mass transfer rate, \dot{M} (g/yr), are the same as used for the modeling of release from the gap (Section 4.1.2), and are not repeated in this section.

The clad portion of the cladding release is modeled using congruent release with corrosion of the zircaloy (Zr) cladding matrix. An approximation for the congruent release of radionuclides (¹⁴C) from the clad, $\dot{M}(cong)$ (g/yr), is as follows:

$$\dot{M}(r,t,cong) = \dot{M}_i(r,t) \frac{\dot{M}_i(R_0,t,cong)}{\dot{M}_i(R_0,t)} \quad (39)$$

where

$$\dot{M}_i(R_0, t, \text{cong}) = \frac{I_i(t)}{I_{Zr}(t)} \dot{M}_{Zr}(R_0, t) \quad (40)$$

and $I_i(t)$ is the time-dependent inventory in the cladding for nuclide i , $I_{Zr}(t)$ is the time-dependent inventory of zircaloy in the cladding, and \dot{M}_i is the solubility-limited diffusive mass transfer rate as calculated using the equations in Section 4.1.1.1.

4.2 Wet-Drip

At the candidate repository site at Yucca Mountain, the anticipated condition is that no liquid should contact most waste packages even after containment failure. Due to local variations in rock permeability, however, water may drip onto a waste package after temperatures have dropped below the boiling point. Assuming that there is a hole near the top of the waste container, the interior of the container may become wet and dissolution of the waste may begin. Release from the waste form can then be estimated based on assumptions about the container. Two types of assumptions are considered in the AREST code. The first assumes that the container is still intact and that release from the waste package cannot occur until the container is filled with water. This assumption is known as the "bathtub" mode. The second mode assumes that the container no longer forms a barrier to transport and thus release can occur at the time of rewetting. This release mode is known as the "flow-through" type. Figure 4.2 shows the models that currently exist in the AREST code to model wet-drip scenarios. The following sections describe the models contained in AREST to estimate release rates under both of these assumptions.

4.2.1 Matrix Release

AREST contains models for both solubility-limited and reaction-rate limited release from the matrix, for the wet-drip environment assuming a bathtub mode (Sadeghi et al. 1990). The next two sections describe these models.

4.2.1.1 Solubility-Limited Advection Model

It is assumed in this model that when the waste form is in contact with the groundwater solubility equilibrium applies. The boundary condition at the waste form surface for each elemental species is, therefore, at a maximum value equal to the solubility of the species. The release rate (\dot{M} , g/yr) is given by:

$$\dot{M}_i(R_1, t) = \begin{cases} 0, & 0 \leq t \leq t_2 \\ C^s \frac{N_i(t)}{N_e(t)} Q, & t_2 \leq t \leq t_3 \\ C^s \frac{N_i(t)}{N_e(t)} Q e^{\left(-\lambda - \frac{Q}{V(t_2)}\right)(t-t_3)}, & t_3 \leq t \end{cases} \quad (41)$$

where C^S is the elemental solubility (g/m^3), N_i and N_e are the species and elemental concentrations in the undissolved solid (g/m^3), respectively, Q is the volumetric flow rate of the groundwater into and out of the container (m^3/yr), t_2 (yrs) is the time in which the container overflows, and t_3 (yrs) is the time at which the element is totally dissolved in the waste form due to the constant waste form dissolution rate.

In AREST, the same equations are used for the bathtub mode and the flow-through mode, except that the time to fill the container (t_2) is different. For the case when the flow-through model is to be used, the time to fill the container is set equal to the time at which water first contacts the waste ($t_2 = t_1$).

4.2.1.2 Reaction-Rate Limited Advection Model

Some of the species in the waste will be soluble enough that solubility constraints do not apply. These species are assumed to be released congruently with the alteration of the waste matrix as it reacts with the groundwater. Two conditions for the alteration-rate limited model, developed at UCB, are considered: 1) the alteration period ($1/f_a$, yrs) is less than the container fill time (t_2) or 2) the alteration period is larger than the fill time. We define f_a , as the fractional alteration rate of the waste matrix, as based on the initial inventory being altered per unit time. In this model, it is assumed that the cylindrical waste form is sitting in a cylindrical container. Water drips into the container and only the submerged portion of the waste form is allowed to alter. In particular, if the alteration time is less than the container fill time, then the bottom part of the waste form is completely altered before the container is filled.

The equations for the mass transfer rate, \dot{M} , when the alteration period is less than the fill time are:

$$\begin{aligned} \dot{M}_i(R_1, t) = & \alpha f_a M^0 \left[\left(\frac{1}{\alpha} + t_1 + \frac{1}{f_a} \right) (e^{\alpha t} - e^{\alpha t_2}) - \left(\frac{e^{\alpha t}}{\alpha} (\alpha t - 1) - \frac{e^{\alpha t_2}}{\alpha} (\alpha t_2 - 1) \right) \right] \\ & + \frac{\alpha e^{-\lambda t_2} M^0}{t_2 - T_1} \left(t_2 - t_1 - \frac{1}{2f_a} \right) e^{(-\lambda - \alpha)(t - t_2)}, \quad t_2 \leq t \leq t_2 + \frac{1}{f_a} \end{aligned} \quad (42)$$

where

$$\alpha = \frac{Q}{V(t_2)} \quad (43)$$

and

$$\begin{aligned} \dot{M}_i(R_1, t) = & \alpha \left\{ e^{(-\lambda - \alpha)\left(t_2 + \frac{1}{f_a}\right)} f_a M^0 \left[\left(\frac{1}{\alpha} + t_1 + \frac{1}{f_a} \right) \left(e^{\alpha\left(t_2 + \frac{1}{f_a}\right)} - e^{\alpha t_2} \right) \right. \right. \\ & \left. \left. - \left(\frac{e^{\alpha\left(t_2 + \frac{1}{f_a}\right)}}{\alpha} \left(\alpha t_2 + \frac{\alpha}{f_a} - 1 \right) - \frac{e^{\alpha t_2}}{\alpha} (\alpha t_2 - 1) \right) \right] \right\} \\ & + \frac{e^{-\lambda t_2} M^0}{t_2 - t_1} \left(t_2 - t_1 - \frac{1}{2f_a} \right) e^{(-\lambda - \alpha)\frac{1}{f_a}} e^{(-\lambda - \alpha)\left(t - t_2 - \frac{1}{f_a}\right)} \quad t_2 + \frac{1}{f_a} \leq t \leq t_3 \end{aligned} \quad (44)$$

where $V(t_2)$ is the volume of the water in the filled container (m^3) and M^0 is the initial inventory of the individual species (g). The flow-through release rate is estimated again by setting the time at which the container will be full (t_2) equal to the time of first wetting (t_1). This assumption again ignores the time it takes the water to react with the waste and dissolve it.

For the case when the alteration period is larger than the time it takes to fill the container, the following equations are used:

$$\dot{M}_i(R_1, t) = f_a M^0 e^{-(\alpha + \lambda)t} \left(e^{\alpha t} - e^{\alpha t_2} \right) + \frac{\alpha}{2} (t_2 - t_1) e^{\alpha t_2} \quad t_2 \leq t \leq t_2 + \frac{1}{f_a} \quad (45)$$

and

$$\dot{M}_i(R_1, t) = f_a M^0 \left(e^{\alpha\left(t_2 + \frac{1}{f_a}\right)} - e^{\alpha t_2} \right) + \frac{\alpha e^{\lambda t_2}}{2} (t_2 - t_1) \quad t_2 + \frac{1}{f_a} \leq t \leq t_3 \quad (46)$$

4.2.2 Gap Release

As with the wet-continuous conditions, there exists the possibility that some of the highly soluble nuclides will dissolve very rapidly when the waste first contacts water. Such nuclides could be located in the gaps or grain boundaries. The equation for the release rate (\dot{M} , g/yr) of the readily soluble species in a wet-drip condition is (Sadeghi et al. 1990):

$$\dot{M}_i(R_1, t) = \alpha \omega M^0 e^{-\lambda t_2} e^{-(\alpha + \lambda)(t - t_2)} \quad t_2 \leq t \quad (47)$$

where ω is the fraction of the inventory that is readily soluble.

4.2.3 Cladding Release

Modeling the release from the cladding of the spent fuel under the wet-drip condition is very similar to modeling cladding under the wet-continuous condition. Modeling the release from the crud uses the same models as release from the gap (Section 4.2.2). Modeling release from the cladding under the wet-drip environment is done with the congruent release models described in Section 4.1.3, except that the release models described in Section 4.2.1.1 are used for the \dot{M} terms.

5.0 Waste-Form Surface Boundary Conditions

One of the main parameters for calculating release from the EBS is the concentration of an element or a radionuclide at the waste form surface. In AREST, we neglect the over pack and assign the surface concentration at the boundary between the container overpack and the backfill. This concentration is modeled several different ways based on the release model or the selection of inputs made by the user. The different methods for determining the surface concentration are discussed in the following sections.

5.1 Input Values

When running AREST, the user has the option to select a constant input value for the solubility limit and thus the surface concentration (C^S) for each nuclide. The user may also, input temperature dependent solubilities for any element. Shared solubilities are used with either method of assigning a solubility limit. Shared solubilities are calculated as the elemental solubility multiplied by the nuclide mass fraction (the nuclide inventory divided by the elemental inventory). These assumptions about time-temperature varying surface concentrations, solubilities, are only valid for the wet-drip release models. The wet-continuous release models were developed for a constant concentration. We have used time-temperature dependent solubilities with the wet-continuous release models, and have found that they yield reasonable results when the solubilities are not drastically different. However, the authors are warning users who may use the time-temperature dependent solubilities with the wet-continuous release models, that the results may not be accurate.

Assuming that the concentration at the waste form surface is limited by the dissolution of the waste (spent fuel or glass), another method of estimating surface concentrations is by the alteration rate of the waste form. This value is input in one of two ways: 1) the length of the alteration, in other words, the length of time during which the waste form is dissolving (Section 4.1.1.4), or 2) the alteration period ($1/f_a$, yrs), estimated as a function of the reaction rate (R_{wf} , g/m²·day), the waste form surface area (S_{wf} , m²), and the total mass of the glass ($mass_{wf}$, g), as:

$$\frac{1}{f_a} = \frac{R_{wf} \cdot S_{wf}}{mass_{wf}} \quad (48)$$

This value is used in the reaction-rate limited release model for the wet-drip conditions (Section 4.2.1.2).

5.2 Glass Dissolution Model

For a glass waste form, AREST contains a model where the surface concentration can also be estimated by considering the coupled reaction between the glass dissolution, an iron overpack, a bentonite clay backfill, and the groundwater (McGrail et al. 1990; McGrail 1991). Consider the heterogeneous dissolution of a glass in a multiphase system consisting of an assemblage of minerals, groundwater and iron that represents the waste package environment. We apply a mass balance on

the system for the parameter ξ (g/m^3), or reaction progress, which is a master variable used to track the overall extent of an irreversible reaction of a solid in water (Aagaard and Helgeson 1982). The mass balance is calculated as follows:

$$\phi V \frac{d\xi}{dt} = s(t) \frac{dX}{dt} - \dot{M}(\xi, R_0, t) \quad (49)$$

where ϕ is the volume fraction of the aqueous phase in an annular volume (V , m^3) surrounding the glass, $s(t)$ (m^2) is the time dependent glass surface area, \dot{M} (g/d) is the mass transfer rate at the waste glass surface, R_0 (cm) is again the radius of the waste container, and dX/dt ($\text{g}/\text{m}^2 \cdot \text{d}$) is the rate at which the glass is dissolving, and is given by:

$$\frac{dX}{dt} = \bar{k} \left(1 - \frac{Q(\xi)}{K} \right) \quad (50)$$

In this equation X ($\text{g}/\text{m}^2 \cdot \text{d}$) is the amount of dissolved glass, \bar{k} ($\text{g}/\text{m}^2 \cdot \text{d}$) is the forward rate of glass dissolution, Q is the ion activity product for an appropriate solid (i.e., chalcedony), and K is the equilibrium constant. The function $Q(\xi)/K$ is calculated as a function of reaction progress by the EQ6 code (Wolery 1983). An example of how to set up the input to EQ6 for an AREST simulation is given in Appendix B. Because silicate glasses are metastable solids in water, the reaction rate is not allowed to go to zero by requiring the following relationship:

$$\frac{dX}{dt} \geq k_r \quad (51)$$

where k_r ($\text{g}/\text{m}^2 \cdot \text{d}$) is a residual rate of reaction (Grambow et al. 1986). The mass transfer rate at the waste glass surface in Equation 49 is calculated using either the wet-continuous solubility-limited model, Section 4.1.1.1, or the numerical transport model, Section 4.1.1.5.

The forward rate of glass dissolution, \bar{k} , is a fundamental property of a silicate glass and depends strongly on glass composition, temperature, and solution pH. In AREST, the following empirical relationships have been implemented to calculate both \bar{k} and k_r as a function of these variables (McGrail 1992):

$$\bar{k} = \hat{k} * 10^{(\eta * \text{pH})} * e^{\left(\frac{E_a}{RT}\right)} \quad (52)$$

$$k_r = \hat{k}_r * 10^{(\eta * \text{pH})} * e^{\left(\frac{E_a}{RT}\right)} \quad (53)$$

where R ($\text{J}/\text{mol}/\text{K}$) is the ideal gas constant. In order to run the glass model option in AREST, the user must input the intrinsic rate constant \hat{k} ($\text{g}/\text{m}^2/\text{day}$), the residual rate constant \hat{k}_r ($\text{g}/\text{m}^2 \cdot \text{day}$), the exponent of hydrogen ion activity (η), and the activation energy E_a (J/mol). Both the temperature T (K) and pH are calculated independently.

Provisions have been implemented in the glass dissolution model to account for the chemical effects of the simultaneous reaction of the glass and iron overpack. The glass-iron interaction is modeled with the aid of the EQ6 geochemical code by adding metallic iron as a special reactant in the input file (see Appendix B). Reaction progress calculations are then run for several cases where the *rk1* parameter in EQ6 is varied for the iron reactant. The *rk1* parameter is calculated as the ratio of moles of iron dissolved per mole of glass dissolved as:

$$rk1 = \frac{\omega(t)}{\xi(t)} \quad (54)$$

where ω is the reaction progress coordinate for the iron. AREST calculates the value of *rk1* at each time step from Equation 54, ξ is calculated from Equation 49, and ω from:

$$\phi V \frac{d\omega}{dt} = A_f(t) \frac{dJ}{dt} - \dot{M}(\omega, R_0, t) \quad (55)$$

where A_f is the inner surface area of the iron overpack (m^2) and dJ/dt is the corrosion rate of the overpack ($g/m^2 \cdot day$). The user of this option must ensure that sufficiently large values of *rk1* have been run so that ω is not exceeded during an AREST simulation. In the current implementation, the iron corrosion rate is simply assigned a constant value as a user input.

For a typical borosilicate waste glass, with approximately 50 wt% SiO_2 , *rk1* values near unity result in low aqueous concentrations of SiO_2 , due to the precipitation of ferrous silicate secondary minerals, such as greenalite. Under these conditions, the glass reaction rate is predicted to be rapid.

6.0 Radionuclide Inventory Models

New models for tracking radionuclide inventories have been implemented in AREST. In particular, models to calculate the exhaustion of radionuclides within the waste form and models to estimate the effect of radioactive decay and in-growth of radionuclides during transport have been implemented. These models are described in the following sections.

6.1 Exhaustion Model

Radioactive decay will eventually lead to depletion of all radionuclides within the waste form. It is important, therefore, that assumptions regarding constant surface concentrations for each nuclide at the waste form surface do not continue if and when each nuclide is exhausted in the waste form.

In the case of alteration-rate limited release, the mass inventory of each nuclide (i.e., nuclide mass fraction) is explicitly evaluated at each time step. Theoretically, some finite mass of each nuclide can be calculated for each succeeding time step; eventually the mass inventories that are calculated would not be physically meaningful. In AREST, an arbitrary cut-off value (e.g., 10^{-10} grams) is set, below which the nuclide is considered to be exhausted in the waste form, and succeeding release calculations are terminated.

For solubility-limited release, the time-dependent mass inventory of each nuclide is also calculated. For this type of release, the surface concentration at the waste form surface is set to a solubility limit. In AREST, a temperature dependent inventory is used to check if there is enough mass of a particular nuclide to sustain a solubility limit. The temperature dependent inventory at a given time, $I(t)$, is compared against its initial inventory, $I(t_0)$. In the current version of AREST, if the time dependent inventory is five orders of magnitude less than the initial inventory then the following relationship is used:

$$\frac{I(t)}{I(t_0)} < 10^{-5} \rightarrow C^s = C^s \frac{I(t)}{I(t_0)} \quad (56)$$

6.2 Decay Chain Models

All actinides are members of a decay chain composed of multiple radionuclides that eventually decay to a stable isotope. Thus, the mass inventory of a given radionuclide, whether in the original waste form or in the groundwater during transport, will be a time-dependent function, affected by loss from radioactive decay and gain by in-growth from a coexisting radioactive parent.

Calculations of mass inventories in the waste form is a straightforward application of Bateman equations to the initial inventories of radionuclides in the emplaced waste. Likewise, the effect of radioactive decay on radionuclide migration in the groundwater away from the waste form has been explicitly incorporated in all of the release models existing in AREST.

The effect of decay chain in-growth on the concentration of migrating radionuclides in groundwater, however, is not specifically incorporated in the existing analytical release models of AREST. An exact analytical equation has been developed for decay chain in-growth (Kang 1990; Pigford et al. 1990), although for completely different set of boundary conditions than are considered in AREST. While new release models for evaluating decay chain in-growth are being developed, it is necessary for the currently implemented models in AREST to approximate the effect of decay chain in-growth.

Modeling the effects of decay chain in-growth utilizes two assumptions: 1) the daughter nuclide will have the same transport properties as its direct parent (e.g., retardation and diffusion coefficient), and 2) because release is evaluated at the backfill/rock interface after diffusional transport through a backfill, secular equilibrium can be assumed to be attained during transit for daughters having much shorter half-lives than their parents. The last assumption only applies for the wet-continuous water contact environment, thus it is only recommended for that type of modeling. The time-dependent release rate of a parent nuclide at the backfill/rock interface is termed \dot{M}_P , and the time-dependent release rate of a daughter at the same location is termed \dot{M}_D , where these values are calculated using activities (Ci). Decay chains are modeled using one of three possible models. The three possible models are described in the following sections.

6.2.1 Long-Lived Parent/Very Short-Lived Daughter

For daughter nuclides with half-lives less than 100 years, it is assumed that the concentration of the daughter nuclide reaching the backfill/rock interface is due entirely to secular equilibrium with the parent. Thus, the following equation is used:

$$\dot{M}_P = \dot{M}_D \quad (57)$$

That is, there is no contribution to the source-term of the short-lived daughter from primary release by the waste form. All of the contribution from the waste form is assumed to have decayed in the transport through the backfill. An example of this case is the decay of ^{237}Np ($t_{1/2} = 2.14 \times 10^6$ years) into ^{233}Pa ($t_{1/2} = 27$ days).

6.2.2 Long-Lived Parent/Short-Lived Daughter

This model is conservatively applied to daughters that have half-lives greater than 100 years. Because the daughter has a half life that is an appreciable fraction of the half life of the parent, the rate of approach to secular-equilibrium must be calculated rather than assumed. The release rate of the daughter at the backfill/rock interface is assumed to be equal to the time-dependent contribution from direct release of the daughter from the waste form, \dot{M}_D^{WF} , plus a time-dependent amount corresponding to the approach to secular equilibrium of the daughter with the parent. This model is illustrated as follows:

$$\dot{M}_D = \dot{M}_D^{WF} + \dot{M}_P(1 - e^{-\lambda_D t}) \quad (58)$$

where λ_D is the decay constant of the daughter. An example of this case is the decay of ^{233}U ($t_{1/2} = 1.59 \times 10^5$ years) into ^{229}Th ($t_{1/2} = 7.34 \times 10^3$ years).

6.2.3 Short-Lived Parent/Long-Lived Daughter

This model was developed to describe the release arising from the decay of a short-lived parent into one or more daughters with successively longer half lives. For the purpose of illustration, assume that the parent (P) decays into a longer-lived daughter (D_1), and that the daughter, in turn, is the parent to another daughter (D_2) that has an even longer half life. The following equation is used to approximate the effect of successive in-growth on the release rate of D_1 :

$$\dot{M}_{D_1} = \dot{M}_{D_1}^{WF} + [\dot{M}_P(\lambda_\infty) - \dot{M}_P(\lambda_P)] \quad (59)$$

This model assumes that the amount of D_1 that reaches the backfill/rock interface is the sum of two contributing parts. The first part of the model is the release rate of D_1 attributable to direct release from the waste form that gets transported across the backfill. The second part of the model is the amount of D_1 that reaches the backfill/rock interface due to radioactive decay of the parent P . This amount is estimated by calculating the release rate of the parent, $\dot{M}_P(\lambda_\infty)$, assuming it is stable (i.e., no loss from radioactive decay), and subtracting the release rate that is calculated from using the actual radioactive decay constant of the parent, $\dot{M}_P(\lambda_P)$.

The calculation of the release rate for D_2 at the backfill/rock interface is more complex. The following equation is used to model the successive in-growth on the release rate of D_2 :

$$\dot{M}_{D_2} = \dot{M}_{D_2}^{WF} + [\dot{M}_{D_1}(\lambda_\infty) - \dot{M}_{D_1}(\lambda_{D_1})] + [\dot{M}_P(\lambda_\infty) - \dot{M}_P(\lambda_P)] \frac{\dot{M}_{D_1}(\lambda_\infty) - \dot{M}_{D_1}(\lambda_{D_1})}{\dot{M}_{D_1}(\lambda_\infty)} \quad (60)$$

The first term in this equation corresponds to the release attributable to the direct release of D_2 . The next term represents the decay of D_1 to D_2 . The last term represents the amount of the parent that decays to D_1 and then decays to D_2 . Longer chains will have an additional term for each additional member of the chain.

7.0 Support Codes

The AREST code requires information about a number of physical, chemical, and nuclear processes. Computer codes that implement detailed models of those processes are often too complex and require too much computational time for them to be included in a probabilistic code such as AREST. In these cases, the actual computer codes are used to make the necessary calculations external to AREST, with the results being input to AREST through lookup tables and transfer functions. The use of external detailed analysis in this fashion preserves the computational efficiency of AREST and also flexibility, since AREST is not tied to a particular model or support code. The support code models and modeling for AREST are briefly discussed in the following sections. Detailed discussion of the support code modeling for AREST is given elsewhere (Altenhofen et al. 1992).

7.1 Thermal Modeling

Temperature can have both a direct and an indirect effect on containment and release performance of the waste package. Waste package temperature profiles are simulated in AREST as described in the original AREST Description Document (Liebetrau et al. 1987). Time dependent temperatures ($T_s(t)$, °C) are simulated based on: 1) an initial heat generation rate simulated from a cumulative distribution ($H_s(0)$, kW/MTU), 2) an initial heat generation rate for the reference container ($H_r(0)$, kW/MTU), 3) a time-temperature distribution for a repository average temperature ($T_a(t)$, °C), and 4) a time-temperature distribution for a reference container temperature ($T_r(t)$, °C). The following equation is used to simulate temperatures in AREST:

$$T_s(t) = \frac{H_s(0)}{H_r(0)}(T_r(t) - T_a(t)) + T_a(t) \quad (61)$$

The HEATING-6 code (Turner et al. 1977) is used to estimate the repository average and the container temperature profiles. These two profiles are read directly into AREST as output from HEATING-6. Temperature histories are used to estimate solubilities, groundwater compositions, and surface concentrations of dissolved glass for the glass dissolution model. Temperatures are estimated for fixed time steps. Linear interpolation is used to estimate temperatures between time steps.

7.2 Geochemical Modeling

The geochemical modeling in AREST includes information relevant to changes in groundwater compositions at different spatial positions within a repository. The speciation/solubility support code, EQ3/6 (Wolery 1983), is used to generate repository groundwater compositions that are read directly into AREST. This same code can be used to estimate elemental solubilities as a function of temperature.

Another utilization of the geochemical modeling occurs with the glass dissolution model of AREST. This model uses a coupled reaction of the glass, groundwater, and iron containers, and the

bentonite backfill. The EQ3/6 code is, again, used to calculate elemental concentrations at the waste form surface as a function of reaction progress and temperature. The elemental concentrations and reaction progress are tabulated by EQ3/6 and read directly into AREST. Also, affinity values for different mineral phases are calculated and tabulated as a function of temperature and reaction progress. The input parameters and setup files for running EQ3/6 for use with the glass dissolution model are discussed in Appendix B. The actual support code files that are read into AREST are discussed in Appendix C.

7.3 Radiological Modeling

Radionuclide inventories are calculated external to AREST, using a source-term code such as ORIGEN-S (Herman and Westfall 1989). The initial inventories, at time of repository closure, are then input into AREST through the input manager and the input data file.

The source-term model, ORIGEN-S, evaluates radionuclide generation and depletion from initial light water reactor operation, through spent fuel reprocessing, interim storage, and repository disposal. The ORIGEN-S code simulates the spent fuel reprocessing step at three years after reactor discharge by extracting a fraction of the elements based on the recovery efficiency.

7.4 Hydrological Modeling

An important part of the modeling of the EBS for a partially saturated zone, such as at the U.S. repository candidate site at Yucca Mountain, Nevada, is the hydrologic modeling. In AREST, parameters such as infiltration rates and saturation values are key parameters that directly affect the calculated performance measures.

The Multiphase Subsurface Transport Simulator (MSTS) computer code has been used to estimate the hydrologic input parameters for AREST. MSTS is a two-phase, two-component, three-dimensional numerical simulator for variably saturated geologic media, with dilute species transport capabilities. MSTS uses a finite-difference-based numerical scheme to solve a nonlinear system of conservation and constitutive equations. The results from MSTS are input to AREST through the input manager and the input data file.

8.0 AREST Code Future

As described in this document, the current version of AREST incorporates a sophisticated user interface to simplify and organize setup and visualization of the computational results. However, we have reached the limits of the capabilities of the fundamental structure of AREST which relies on relatively simple analytical models to describe release and transport of radionuclides in the EBS. Within the next few years, the Yucca Mountain Project will be examining alternative EBS concepts that cannot be analyzed with the current version of AREST. Consequently, a fundamental restructuring of AREST is needed to implement robust but computationally efficient numerical models for EBS performance analysis.

We propose that the next generation of AREST be based on a two-dimensional finite volume method for solving chemical reactive transport problems with capabilities for handling constant, time-varying, and periodic boundary conditions. This capability is particularly important for modeling stochastic flow in fractures that may intersect a waste package, as speculated for the candidate site for the U.S. repository at Yucca Mountain. An orthogonal grid will be used for the spatial discretization with provisions to implement a three-dimensional non-orthogonal grid in the future. The model will explicitly handle n-member decay chains and will enforce solubility constraints throughout the spatial domain.

9.0 References

- Aagaard, P., and H. C. Helgeson. 1982. "Thermodynamic and Kinetic Constraints on Reaction Rates Among Minerals and Aqueous Solutions. I. Theoretical Considerations." *American Journal of Science* 282:237-285.
- Altenhofen, M. K., A. S. Koontz, K. I. Johnson, E. C. Kohler, and D. W. Damschen. 1992. "Near-Field Support Codes for AREST-PNC: The Analytical Repository Source-Term Model-PNC System Version." In *Performance Assessment Center for Engineered Barriers (PACE) Program FY 1991 Summary Report*, PNC PA0865 92-001, prepared by Battelle, Pacific Northwest Laboratories for PNC, Tokoyo, Japan.
- Benedict, M., and T. H. Pigford. 1957. *Nuclear Chemical Engineering*. McGraw-Hill, New York.
- Engel, D. W., A. M. Liebetrau, G. C. Nakamura, B. M. Thornton, and M. J. Apted. 1989. *The AREST Code: User's Guide for the Analytical Repository Source-Term Model*. PNL-6645, Pacific Northwest Laboratory, Richland, Washington.
- Engel, D. W., B. P. McGrail, K. Worgan, and M. J. Apted. 1992. "AREST-PNC Model Description." In *Performance Assessment Center for Engineered Barriers (PACE) Program FY 1991 Summary Report*, PNC PA0865 92-001, prepared by Battelle, Pacific Northwest Laboratories for PNC, Tokoyo, Japan.
- Grambow, B. E., H. P. Hermansson, I. K. Bjorner, H. Christensen, and L. Werme. 1986. "Reaction of Nuclear Waste Glass with Slowly Flowing Solutions." In *Advances in Ceramics - Volume 20: Nuclear Waste Management II*, eds. D. E. Clark, W. B. White, and A. J. Machiels. American Cermaic Society, Inc., Westerville, Ohio.
- Grindrod, P., M. Williams, M. Impey, and H. Grogan. 1991. *STRENG: A Source Term Model for Vitrified High Level Waste*. Technical Report NTB 90-48, NAGRA, Wettingen, Switzerland.
- Herman, O. W., and R. M. Westfall. 1989. *ORIGEN-S: Scale System Module to Calculate Fuel Depletion, Actinide Transmutation, Fission Product Building and Decay, and Associated Radiation Source Terms*. NUREG/CR-0200, Vol. 2, Sec. F7, prepared by Oak Ridge National Laboratory for the U.S. Nuclear Regulatory Commission, Washington, D.C.
- Hwang, Y., and T. H. Pigford. 1990. *Life of Copper Canister Limited by Mass Transfer of Sulfide*. UCB-NE-4167, University of California at Berkeley, Berkeley, California.
- Kang, C.-H. 1990. *Mass Transfer and Transport of Radionuclides through Backfill in a Geologic Nuclear Waste Repository*. Doctoral Dissertation Thesis, University of California at Berkeley, Berkeley, California.

Liebetrau, A. M., M. J. Apted, D. W. Engel, M. K. Altenhofen, D. M. Strachan, C. R. Reid, C. F. Windisch, R. L. Erickson, and K. I. Johnson. 1987. *The Analytical Repository Source-Term (AREST) Model: Description and Document*. PNL-6346, Pacific Northwest Laboratory, Richland, Washington.

McGrail, B. P. 1991. "Modeling Release From Borosilicate Glass." In *Performance Assessment Center for Engineered Barriers (PACE) Program FY 1990 Summary Report*, PNC PA0865 91-001, prepared by Battelle, Pacific Northwest Laboratories for PNC, Tokoyo, Japan.

McGrail, B. P. 1992. "Modeling Release From Borosilicate Glass Under Open-System Conditions." In *Performance Assessment Center for Engineered Barriers (PACE) Program FY 1991 Summary Report*, PNC PA0865 92-001, Battelle, Pacific Northwest Laboratories for PNC, Tokoyo, Japan.

McGrail, B. P., M. J. Apted, D. W. Engel, N. Sasaki, and S. Masuda. 1990. "A Coupled Chemical-Mass Transfer Submodel for Predicting Radionuclide Release from an Engineered Barrier System Containing High-Level Waste Glass." In *Science Basis for Nuclear Waste Management XII*, Materials Research Society, Pittsburgh, Pennsylvania.

Nakamura, G. C., and M. L. Wilkins. 1992. "AREST-PNC User's Guide." In *Performance Assessment Center for Engineered Barriers (PACE) Program FY 1991 Summary Report*, PNC PA0865 92-001, prepared by Battelle, Pacific Northwest Laboratories for PNC, Tokoyo, Japan.

Pigford, T. H., P. L. Chambré, and W.W.-L. Lee. 1990. *A Review of Near-Field Mass Transfer in Geologic Disposal Systems*. LBL-27045, Lawrence Berkeley Laboratory, Berkeley, California.

Sadeghi, M. M., T. H. Pigford, P. L. Chambré, and W.W.-L. Lee. 1990. *Equations for Predicting Release Rates for Waste Packages in Unsaturated Tuff*. LBL-29254, Lawrence Berkeley Laboratory, Berkeley, California.

Turner, W. D., D. C. Elrod, and I. I. Siman-Tov. 1977. *HEATINGS5—An IBM 360 Heat Conduction Program*. ORNL/CSD/TM-15, Oak Ridge National Laboratory, Oak Ridge, Tennessee.

Wolery, T. J. 1983. *EQ3/6 A Computer Program for Geochemical Aqueous Speciation-Solubility Calculations User's Guide and Documentation*. UCRL-53414, Lawrence Livermore National Laboratory, Livermore, California.

Appendix A

Release Model Verification

Appendix A

Release Model Verification

AREST was designed to implement release models in such a way that the user can select the release mode and release model for each analysis. In doing so, all of the release models are modules/subroutines that can be removed or added with minor difficulties. In AREST, there are several release models, as described in Section 4.0, that were developed elsewhere (UCB and Intera) and implemented as needed. The verification that the models accurately calculate the correct results is done primarily by comparing the results from AREST to results that have been published by the developers of the release models.

Figures A.1 through A.12 contain plots of results from AREST analyses. The AREST results in these figures are always represented by solid lines, while comparable results from the developers' documentation are represented with an "x". The actual data for these comparison/verification runs are not listed in this appendix since they are described in the original documents which describe the release models created by the developers.

For example, Figure A.1 shows the AREST results when using the solubility-limited release model, with diffusive transport through a backfill, and release into a porous host rock (PDS model). This model is used in a "wet-continuous" water contact mode. These results compare favorably with results published by the UCB group (Chambré et al. 1985, Figure 5). In this plot, Figure A.1, the solid line represents the results from AREST while the published results, for which the AREST results are compared, are shown with an "x". The differences beyond 10^5 years for the nuclide with the shorter half life (5730 years) occur because AREST uses an exhaustion model, described in Section 6.1.

Figure A.2 shows results for the steady-state mass transport model (PCS), assuming a solubility-limited boundary condition at the waste form with diffusive transport through a backfill and diffusive/advective release into a porous host rock (Pigford et al. 1990). This model is used in a "wet-continuous" water contact model. This model is verified using hand calculations. The input routine for AREST for the verification of this model is shown in Table A.1.

The verification results for the fissure/fracture release model are shown in Figure A.3. The AREST results are again compared to published results (Kang 1990, Figure 4.14). These results are from a model that assumes: 1) solubility-limited concentrations, 2) diffusive transport through a backfill, 3) convective release into a fractured rock, and 4) a "wet-continuous" water contact mode (FCS). The results compare quite well, with minor discrepancies occurring in the early time frame due to differences in the numerical techniques and approximations.

Good agreement also occurs with the verification of the alteration-limited release model (PDR) in a "wet-continuous" water contact mode, Figure A.4. The AREST results (solid line) are compared against results from UCB (Sadeghi et al. 1990, Figure 29).

The numerical transport model that has been implemented in AREST was verified against analyses from the STRENG model. Figure A.5 shows a comparison for the neptunium decay chain (Grindrod et al. 1991, Figure 15). Again, good agreement is accomplished with the discrepancy for ^{241}Am occurring because of the exhaustion model in AREST.

Figure A.6 shows the results from the inventory-limited/gap release model. These results are from a "wet-continuous" water contact mode. The comparison to results from UCB (Kang 1990, Figure 3.8) is again quite good. In this comparison, it is assumed that the container fails 1000 years after repository closure. This data is not provided in the UCB document, but with trial and error this value was found to work quite well.

The verification for the "wet-drip" release models are shown in Figures A.7, A.8, and A.9. These results are all compared against results from UCB (Sadeghi et al. 1990). Figure A.7 shows the effect of shared solubilities for the plutonium nuclides and is compared against the UCB results (Sadeghi et al. 1990, Figure 1). Figure A.8 shows a good comparison with published results (Sadeghi et al. 1990, Figure 7) for the alteration-limited release model assuming a "wet-drip" water contact mode. Minor discrepancies occur in the results for the inventory-limited/gap release model shown in Figure A.9. The AREST results are compared to Figure 6 from Sadeghi et al. 1990. The differences occur in the estimation of the void volume for the two models. A difference in the volume will cause a difference in the fill-up time and also the concentration estimate for release.

The last three plots show runs for the glass dissolution model (see Section 5.0). Figure A.10 shows the results of a base case analysis where the glass dissolution model is not utilized. Instead, the concentrations at the waste form surface are limited by the solubility for each nuclide. The numerical transport model was used for this analysis. These results compared quite well with another numerical transport model, RELEASE (McGrail 1992, Section 2A, Figure 9).

Figure A.11 shows results from the same analysis as shown in Figure A.10, except that the glass dissolution model in AREST is used. This analysis ignores the effects of the corrosion products and their reaction with the glass waste form. Figure A.12 shows the results of using the glass dissolution model and the effects of considering the iron corrosion products and the reaction with the glass waste form. The data files that are used by the glass dissolution model for the affinities and concentrations are very large files. Thus, it is beyond the scope of this document to display the data files and the complex sequence of steps to verify the glass dissolution model.

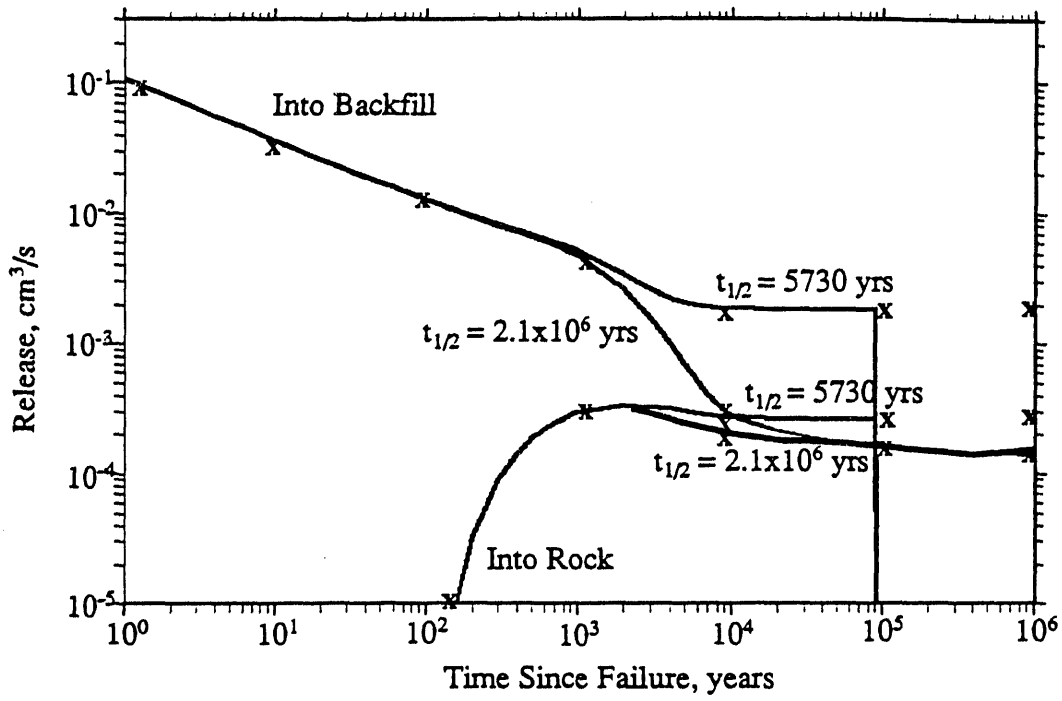


Figure A.1. Verification Plot for the PDS Matrix Release Model (UCBMAT)

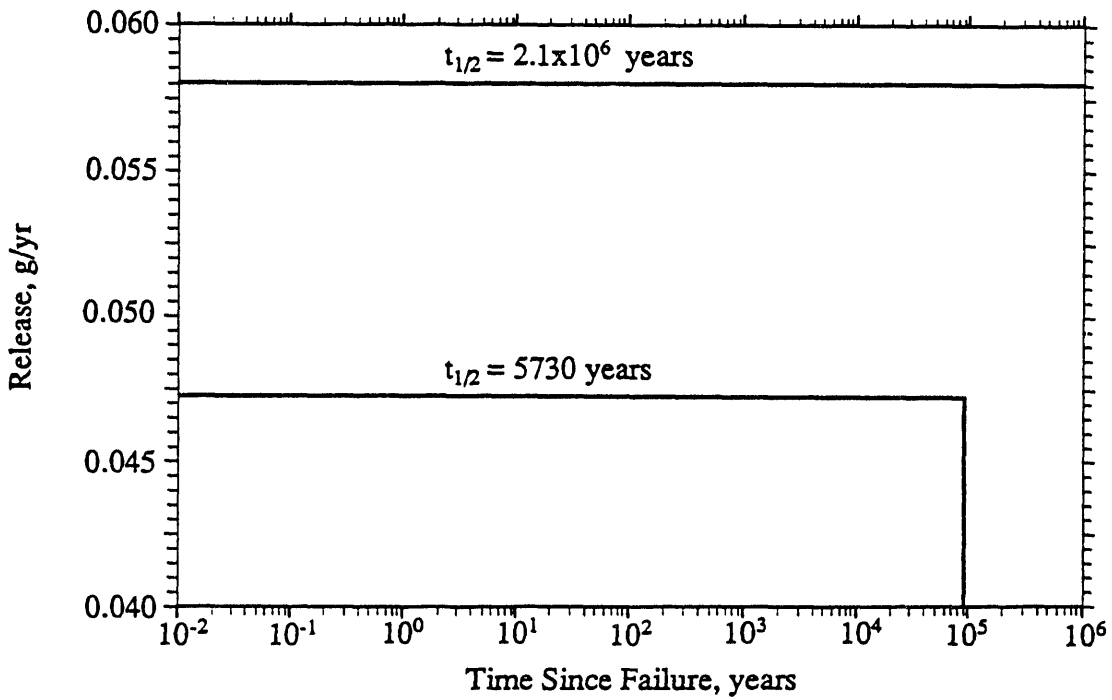


Figure A.2. Verification Plot for the PCS Matrix Release Model (UCBCONV)

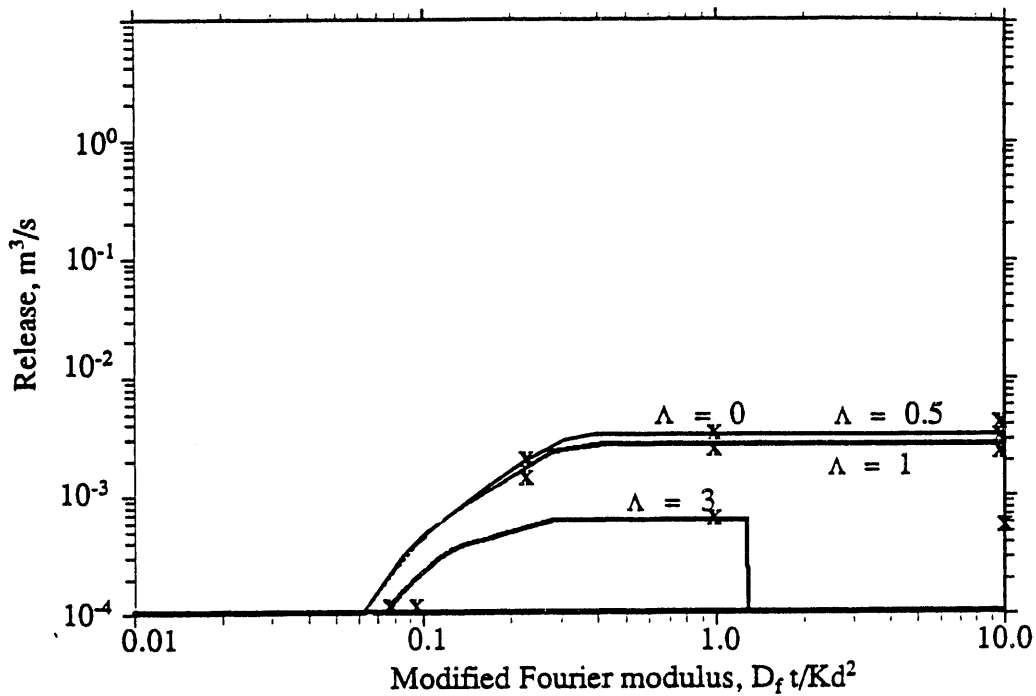


Figure A.3. Verification Plot for the Fissure/Fracture Matrix Release Model (UCBFISS)

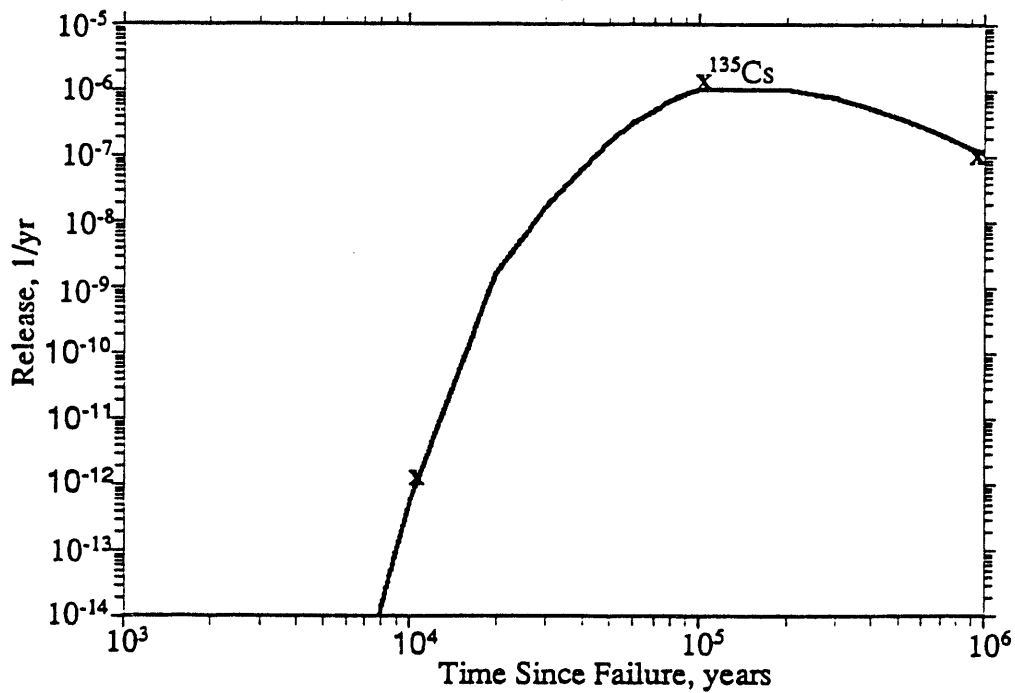


Figure A.4. Verification Plot for the PDR Matrix Release Model (UCBALT)

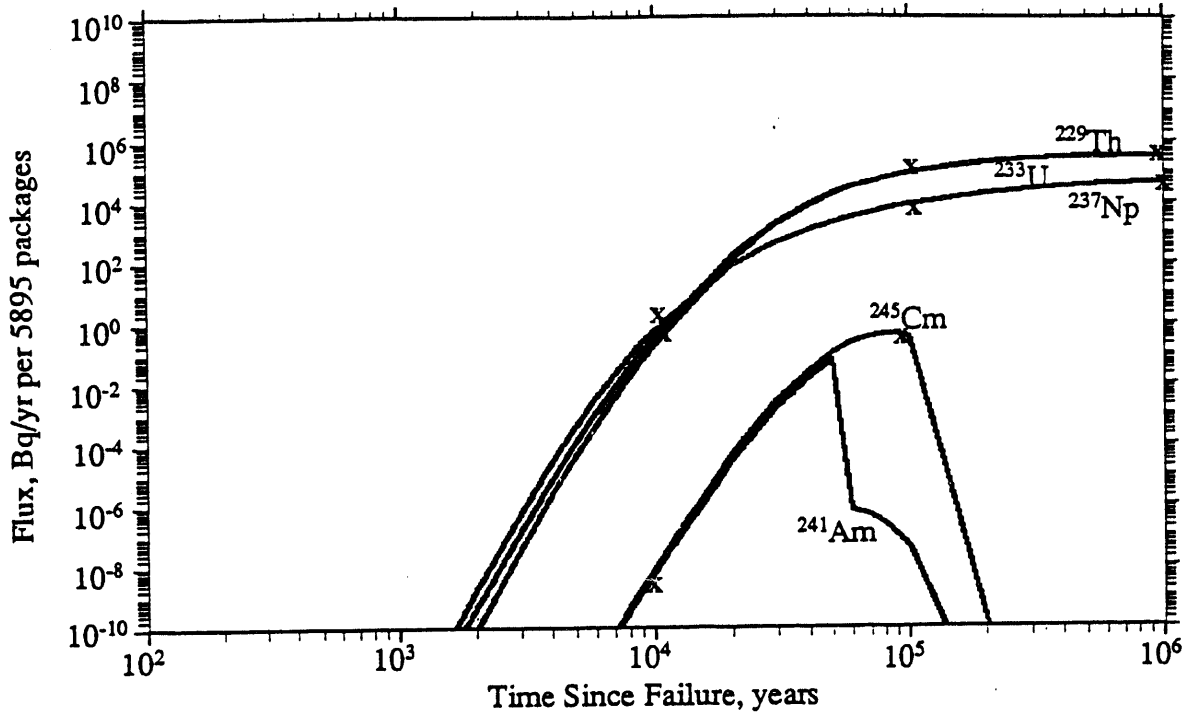


Figure A.5. Verification Plot for the Numerical Release Model (STRENG)

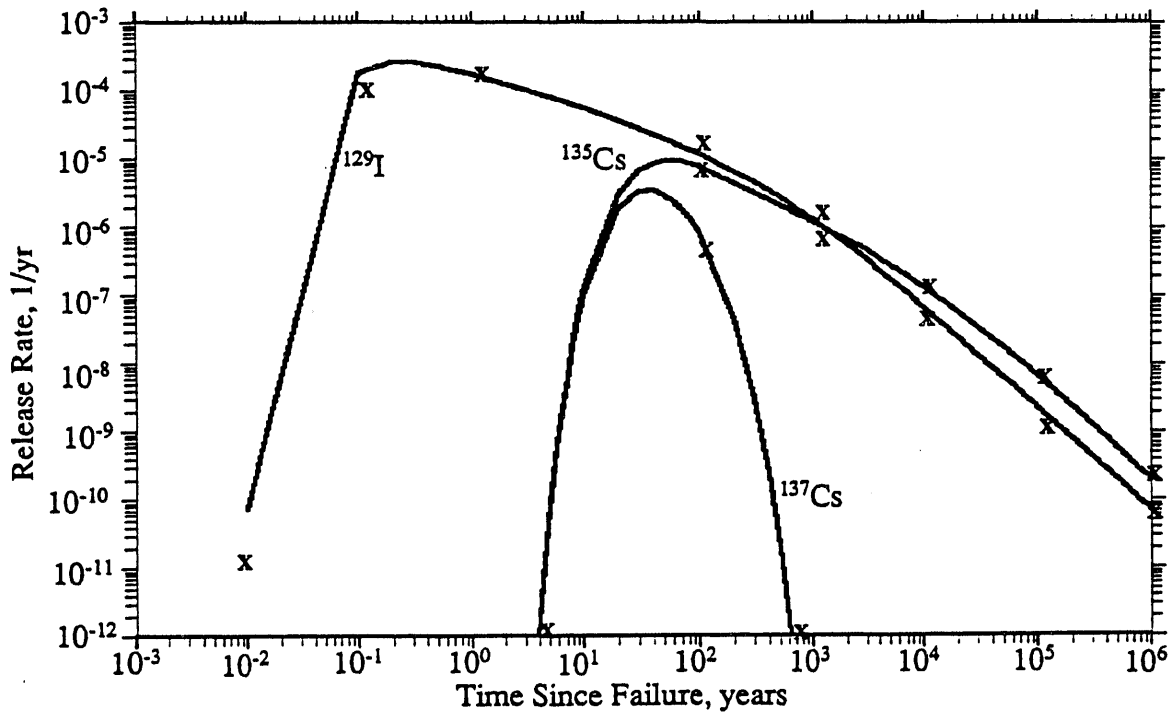


Figure A.6. Verification Plot for the Inventory-Limited/GAP Release Model (UCBGAP)

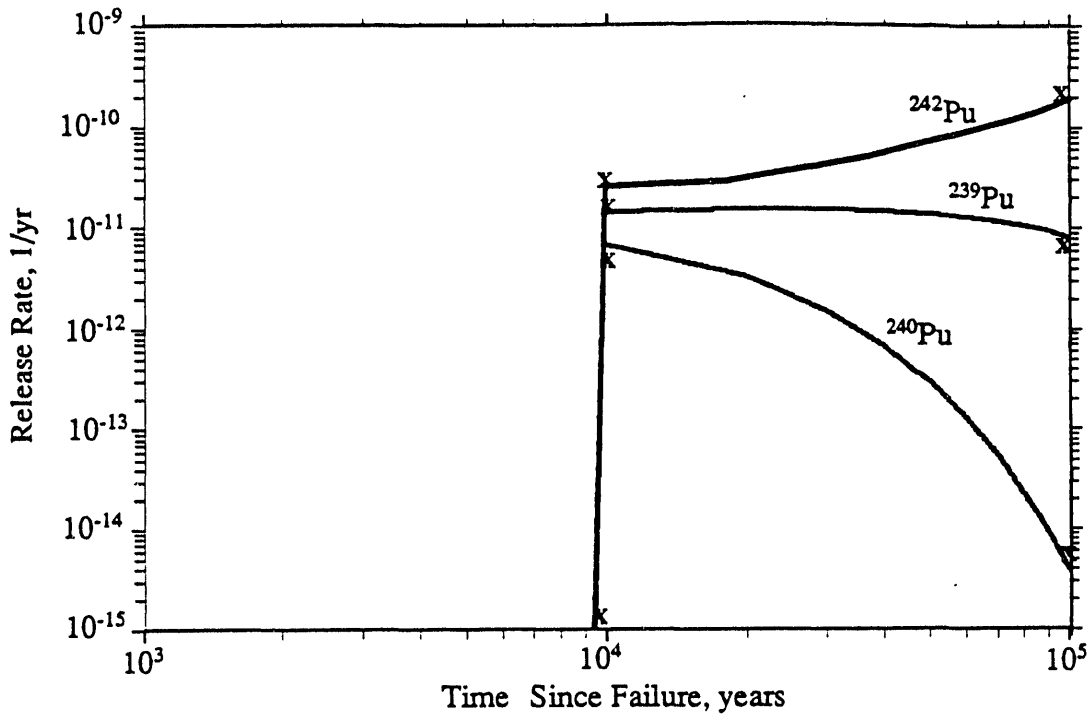


Figure A.7. Verification Plot for the Solubility-Limited Release Model for "Wet-Drip"

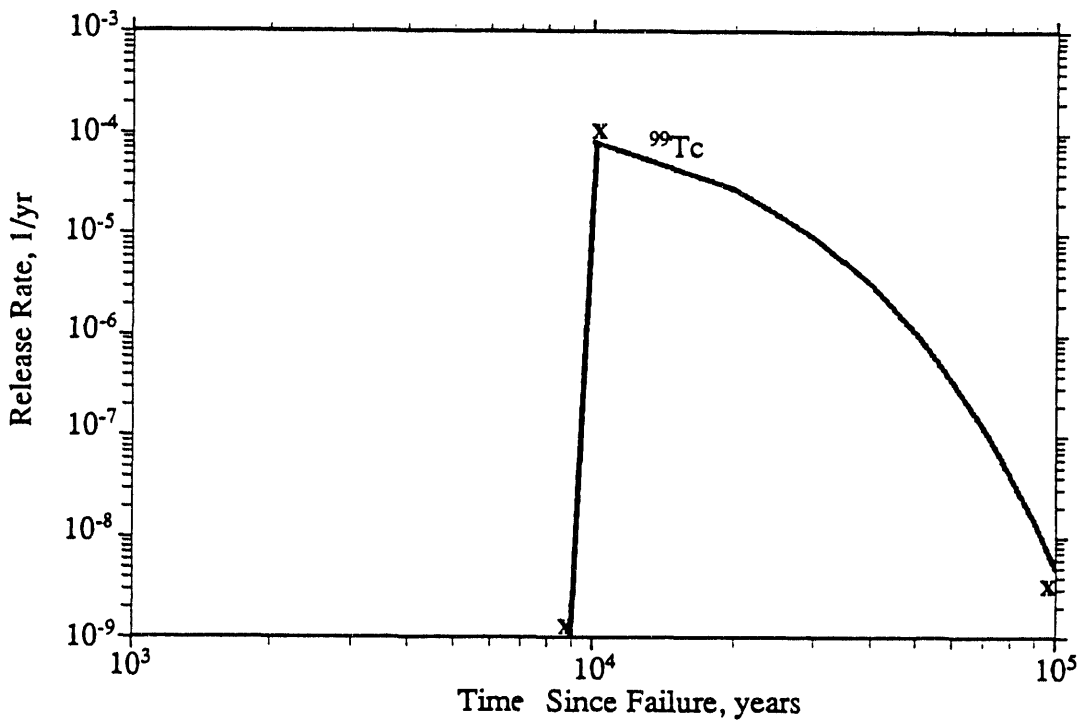


Figure A.8. Verification Plot for the Alteration-Limited Release Model "Wet-Drip"

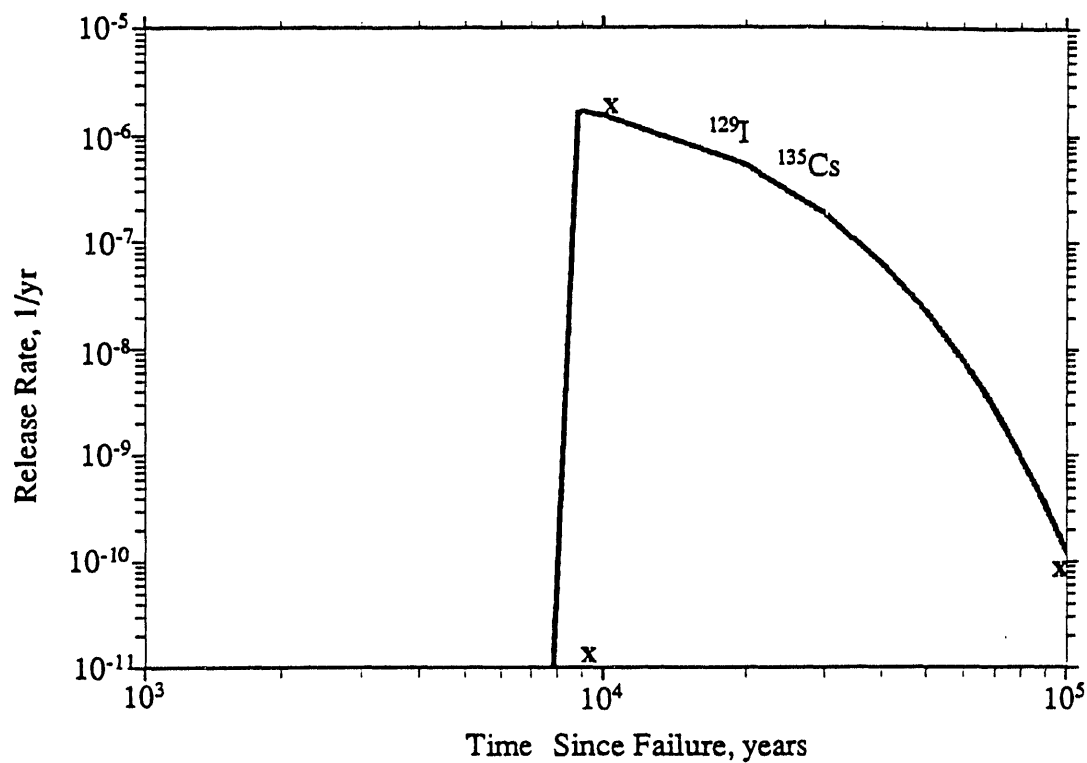


Figure A.9. Verification Plot for the Inventory-Limited/Gap Release Model for "Wet-Drip"

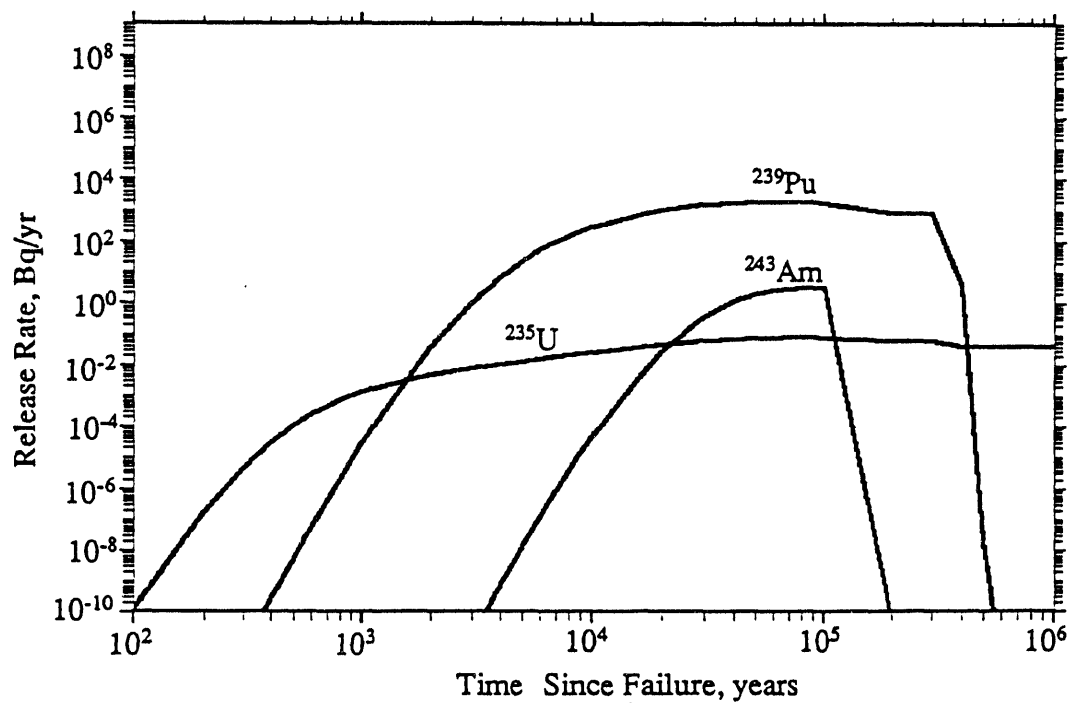


Figure A.10. Base Case for Comparing with Glass Dissolution Model

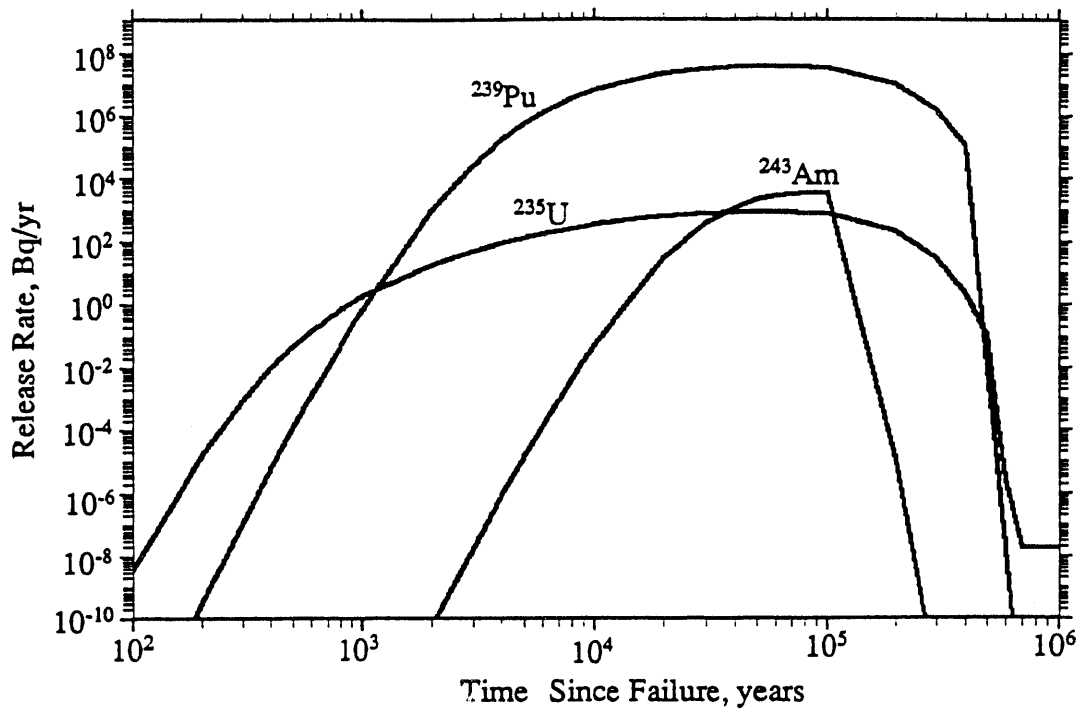


Figure A.11. Plot for the Glass Dissolution Model Not Considering Iron Corrosion

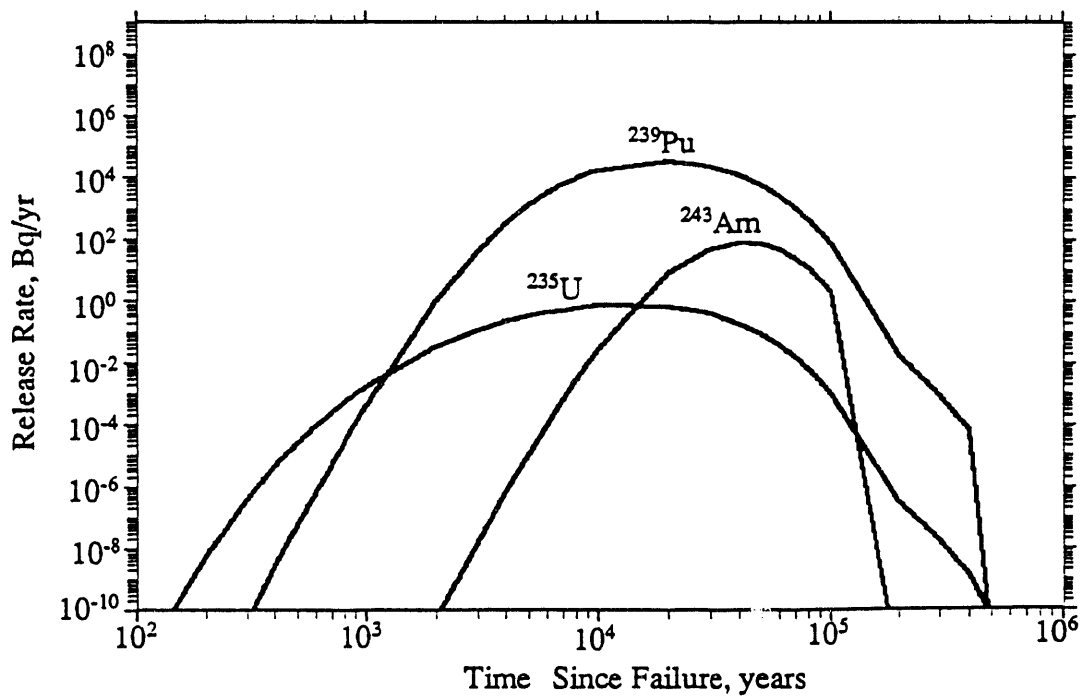


Figure A.12. Plot for the Glass Dissolution Model Considering Iron Corrosion

Table A.1. AREST Input Data File for the Verification of the Diffusive/Advective Release Model (PCS)

```

! AREST-PNC Data Input File
! ID      :
! Date    : Tue Oct  8 16:06:42 1991

#BLOCK Simulation_Control
  0  ! Type of sensitivity analysis
      ! 0 = None
      ! 1 = Base-alternate
      ! 2 = Full factorial
  1  ! No. of sensitivity analysis cases
  1  ! Samples per distribution
  0  ! Seed for random number generation
  1  ! Total simulations
#ENDBLOCK Simulation_Control

! Run identification
Convective Release Model (UCBCONV)      ! run title

#BLOCK time-temp/heat
#INCLUDE support/pnc_ref_temp.dat      ! timetemp file
#INCLUDE support/pnc_min_temp.dat      ! timetemp file
#INCLUDE support/pnc_hl.dat            ! heatload file

  500.000000      ! resaturation temperature
  1.100000      ! heat load conversion
#ENDBLOCK time-temp/heat

#BLOCK solubility
#INCLUDE support/solubility.dat        ! solubility file
#ENDBLOCK solubility

#BLOCK groundwater
#INCLUDE support/pnc_envsol.dat        ! groundwater file
#ENDBLOCK groundwater

#BLOCK waste_package_design
  29.0      ! Cylindrical waste radius      cm
  476.0     ! Cylindrical waste length      cm
  17.8      ! Cylindrical waste form radius  cm
  470.0     ! Cylindrical waste form length  cm
  5.0       ! Waste container thickness     cm
  30.0      ! Backfill thickness            cm
  1         ! Container emplacement type
      ! 0 --> Vertical emplacement
      ! 1 --> Horizontal emplacement
  391.0     ! Container/WP spacing/height     cm
#ENDBLOCK waste_package_design

#BLOCK containment
  1000.000000 ! time of failure
  0.000000    ! prefailure probability
  0           ! initial prefailures
#ENDBLOCK containment

! Release control
-1           ! release control

```

```

#BLOCK release
      8          ! release model
False      ! congruent release
1.000000   ! release fractional distance
      1.0       ! packing tortuosity
      1.0000   ! host rock tortuosity
      1.8       ! packing density (g/cm^3)
      3.0000   ! host rock density (g/cm^3)
      100.0     ! percentage of pores filled
      1.000000 ! glass cracking factor
      3.36e4    ! wasteform mass (g)
      0.5       ! waste void width (cm)
      1.0       ! waste void volume factor
False      ! precipitation
False      ! solubility limited
False      ! shared solubility
False      ! Glass dissolution model being used?
      1         ! Calculating release rates or concentrations
          !           1 --> release rates
          !           -1 --> Conc. vs. time (distance curves)
          !           -2 --> Conc. vs. distance (time curves)

#BLOCK release_model_parameters

#BLOCK solubility_model
      0.2000    ! packing porosity
      0.010000 ! host rock porosity
#ENDBLOCK solubility_model

#BLOCK convection_model
      1.316     ! pore water flow rate (m/yr)
      0.1       ! packing porosity
      0.1       ! host rock porosity
#ENDBLOCK convection_model

#ENDBLOCK release_model_parameters

#ENDBLOCK release

#BLOCK precipitation
      1.000000   ! precipitation fractional distance
      1.000000   ! precipitation fractional concentration
#ENDBLOCK precipitation

#BLOCK misc_control
      False      ! vector approach
      1          ! Input inventory units (1 --> g/yr, 2 --> Ci/yr)
#ENDBLOCK misc_control

#BLOCK radionuclides

#BLOCK nuclide_name
      Pu-240     ! nuclide name
      Np-237     ! nuclide name
#ENDBLOCK nuclide_name

#BLOCK daughter_product
      none       ! daughter product
      none       ! daughter product
#ENDBLOCK daughter_product

```

```

#BLOCK halflife
  5.73E+03      ! halflife      years
  2.10E+06      ! halflife
#ENDBLOCK halflife

#BLOCK inventory
  50000000.000000 ! inventory      g/pack
  50000000.000000 ! inventory
#ENDBLOCK inventory

#BLOCK solubility
  1.0           ! solubility      g/m^3
  1.0           ! solubility
#ENDBLOCK solubility

#BLOCK kd1
  111.0         ! kd1             ml/g
  111.0         ! kd1
#ENDBLOCK kd1

#BLOCK kd2
  3.33          ! kd2             ml/g
  3.33          ! kd2
#ENDBLOCK kd2

#BLOCK diffusion
  0.000010     ! diffusion        cm^2/s
  0.000010     ! diffusion
#ENDBLOCK diffusion

#BLOCK matrix_percentage
  100.0
  100.0
#ENDBLOCK matrix_percentage

#BLOCK gap_percentage
  0.0
  0.0
#ENDBLOCK gap_percentage

#BLOCK clad_percentage
  0.0
  0.0
#ENDBLOCK clad_percentage

#BLOCK crud_percentage
  0.0
  0.0
#ENDBLOCK crud_percentage

#ENDBLOCK radionuclides

#BLOCK overall_control
  1             ! repository waste packages
#ENDBLOCK overall_control

```

References

- Chambré, P. L., T. H. Pigford, W.W.-L. Lee, J. Ahn, S. Kajiwara, C. L. Kim, H. Kimure, H. Lung, W. J. Williams, and S. J. Zavoshy. 1985. *Mass Transfer and Transport in a Geologic Environment*. LBL-19430, Lawrence Berkeley Laboratory, Berkeley, California.
- Grindrod, P., M. Williams, M. Impey, and H. Grogan. 1991. *STRENG: A Source Term Model for Vitrified High Level Waste*. Technical Report NTB 90-48, NAGRA, England.
- Kang, C.-H. 1990. *Mass Transfer and Transport of Radionuclides through Backfill in a Geologic Nuclear Waste Repository*. Doctoral Dissertation Thesis, University of California at Berkeley, Berkeley, California.
- McGrail, B. P. 1992. "Modeling Release From Borosilicate Glass Under Open-System Conditions." In *Performance Assessment Center for Engineered Barriers (PACE) Program FY 1991 Summary Report*, PNC PA0865 92-001, prepared by Battelle, Pacific Northwest Laboratories for PNC, Tokoyo, Japan.
- Pigford, T. H., P. L. Chambré, and W.W.-L. Lee. 1990. *A Review of Near-Field Mass Transfer in Geologic Disposal Systems*. LBL-27045, Lawrence Berkeley Laboratory, Berkeley, California.
- Sadeghi, M. M., T. H. Pigford, P. L. Chambré, and W.W.-L. Lee. 1990. *Predictions of Release Rates for a Waste Repository at Yucca Mountain*. LBL-27767, Lawrence Berkeley Laboratory, Berkeley, California.

Appendix B

Geochemical Data Input for Glass Model

Appendix B

Geochemical Data Input for Glass Model

The purpose of this Appendix is to provide a description and examples of the steps needed to assemble the input data to run the glass dissolution model in the AREST code. These steps are broken down as follows:

- EQ3NR Input and Generation of Pickup file
- EQ6 Input
- EQ6 Output
- Modeling Glass-Iron Interactions.

It should be emphasized here that the following description is **not** a substitute for the EQ3/6 user manuals and it has been assumed that the user is thoroughly familiar with the basic operation of the EQ3/6 code package.

EQ3NR Input and Generation of Pickup File

Prior to running any reaction path calculation with the EQ6 code, the EQ3NR code must be run to generate an appropriate "pickup" file which is appended to the EQ6 input file. An example input file is shown in Table B.1. All radioelements and major glass components that are of interest for study in an AREST simulation should be included in this file. We have arbitrarily set the starting concentration for the basis species to 10^{-15} molar in this example. This would be appropriate for a simulation of the glass reaction in deionized water. The initial concentrations of the major cations and anions in a starting groundwater could also be entered in place of these values. The user is cautioned here about entering every possible element present in either the glass, groundwater, or both. The computational time required for the subsequent EQ6 runs can increase dramatically as the number of elements to be considered increases. The user should consider removing those trace constituents that have little impact on the solution chemistry or resulting elemental solubilities.

A second feature that is important in this example is the redox couple used to indirectly constrain the O_2 fugacity. In this case, the Fe^{++}/Fe^{+++} couple has been selected by setting the $uredox=fe+++$. We have also established redox equilibrium by constraining the Fe^{++} activity by equilibrium with magnetite, and the Fe^{+++} activity by equilibrium with hematite. The reader should note, however, that this fixes only the initial O_2 fugacity since the EQ6 code calculates this parameter as a function of reaction progress.

EQ6 Input

After completing the appropriate EQ3NR run as described above, the next step is to create an input file for the reaction path calculations with the EQ6 code. An example input file is shown in Table B.2 where the EQ3NR pickup file has been removed from the bottom of the file. Because AREST uses an interpolation algorithm for all the computations using the geochemical data, the user must ensure that a sufficient range of temperature is covered for the simulations that are to be run with AREST. This entails executing separate runs of the EQ6 code for a series of selected temperatures.

One of the key parameters in the input file (Table B.2) is *zimax*. This parameter dictates the maximum value of reaction progress that is to be simulated. It is very important that a sufficiently large value of reaction progress be selected that will not be exceeded during an AREST simulation. If the user specifies certain chemical or mass transport conditions that cause calculated reaction progress values to exceed the input data, the AREST calculation will be terminated at that point. One way to ensure that this does not happen is to check for saturation with respect to the mineral phase that will be used to control the reaction kinetics of the glass. Some appropriate phases include amorphous silica or chalcedony. Because the reaction affinity is very sensitive to undersaturation, and mass transfer rates are usually small for a diffusion dominated system, reaction progress values can become quite large if proper care is not exercised in the selection of mineral phases for kinetic rate control.

The second important parameter in the input file is the option to fix gas fugacities, in particular $O_2(g)$. In most instances it is desirable to allow the EQ6 code to calculate the oxygen fugacity as a function of the various chemical equilibria involved in the system. However, the user should be aware that when simulating the dissolution of a glass, the oxygen liberated from the breakup of the glass network is usually sufficient to drive the system oxidizing, irrespective of the initial conditions assumed. This effect can be circumvented by fixing the oxygen fugacity at a low value, or by simulating the simultaneous reaction of iron which consumes the oxygen liberated by glass dissolution through oxidation-reduction reactions. However, the simultaneous reaction of iron also has other important chemical effects that are discussed below.

The third important part of the EQ6 input file is the so called special reactant section, which is used to input the bulk chemical composition of the glass (and other reactants) for reaction path simulations. A spreadsheet template has been created to automate the calculations required to convert a glass composition, usually given in oxide wt%, to the elemental mole fractions needed for input as a special reactant in EQ6.

EQ6 Output

The EQ6 code normally produces a very large file called "output" that contains detailed information on the solution chemistry and secondary mineral formation as a function of reaction progress. A compressed version of the data in the output file is also generated in a "tab" file that contains element concentrations as a function of reaction progress in a tabular form, as well as details on the identity and amount of secondary phases formed during the simulation. Unfortunately, the

information necessary to run the glass dissolution model is not provided in either the standard "output" or "tab" files produced by EQ6. Consequently, we have modified EQ3/6 to produce a series of support files called "*.arest".

Of particular importance for glass dissolution modeling are the files "affinity.arest" and "conc.arest". The "affinity.arest" file contains the calculated affinities as a function of reaction progress for all the minerals loaded into memory at the start of an EQ6 run. The user is required to input a mineral name from this list that will be used to control the reaction kinetics during an AREST simulation. The "conc.arest" file contains a compact listing of the element concentrations as a function of reaction progress that, are used to determine the time-dependent concentrations at the waste form surface during an AREST simulation. The "minerals.arest" file produces a tabular listing of the identity and amount of secondary phases formed. Although this data is not used in AREST, it provides important information to identify the solubility-limiting phase(s), if any, that fix the boundary condition at the waste form surface for subsequent transport. The last file generated is the "groundh2o.arest" file which contains a listing of aqueous species as a function of reaction progress. Again, this file is not directly used in the current version of AREST but has been provided for possible future use in models that require aqueous speciation data, e.g., Cl^- concentrations for a corrosion model.

Modeling Glass-Iron Interactions

Some waste package designs include massive cast steel overpack to provide structural support and containment of the waste for some period of time after emplacement. Because a number of laboratory studies have shown a strong synergistic effect of iron corrosion on glass dissolution, we have included provisions in AREST to model these effects. The approach taken is to modify the input to EQ6 to include Fe^0 as a special reactant in addition to the glass itself (see Table B.2). Including Fe^0 in the calculations not only affects the solution Eh through oxidation-reduction reactions but also the reaction affinity for dissolution of the glass itself, as illustrated in Figure B.1. As increasing amounts of iron are added per mole of glass reacted (larger rk1 values), the system is driven into the stability region for greenalite precipitation, which lowers the activity of orthosilicic acid and thereby increases the driving force for glass dissolution. For the purposes of an AREST simulation, an additional set of EQ6 calculations must be run, with progressively increasing rk1 values for the Fe^0 special reactant. The user must also ensure that a sufficient range of reaction progress and rk1 values have been covered so that these values will not be exceeded during an AREST simulation.

Table B.1. Example Input File for EQ3NR

input file name= p0798.eq3.inp created= 05-DEC-91 creator= B.P. McGrail

This run will calculate the starting water composition for EQ6 simulations of the reaction of p0798 glass in deionized water. The starting water is not equilibrated at 25C with air. Starting glass components are set at 10^{-15} molar.

```

endit.
  tempc=          25.
  rho=           1.00      tds pkg=          0.      tds spl=          0.
  fep=
  tolbt=          0.      uredox=fe+++
  itermx= 0          toldl=          0.      tolsat=          0.
  iopt1-10=      1      0      0      0      0      0      0      0      0      0
  iopgl-10=      0      0      0      0      0      0      0      0      0      0
  iopr1-10=      0      0      0      0      0      0      0      0      0      0
  iopr11-20=     0      0      0      0      0      0      0      0      0      0
  iodbl-10=     0      0      0      0      0      0      0      0      0      0
  uebal= h+
  uacion=
  nxmod= 3
  species= tridymite
  type= 1          option= -1          xlkmod=          0.
  species= cristobalite
  type= 1          option= -1          xlkmod=          0.
  species= quartz
  type= 1          option= -1          xlkmod=          0.
data file master species= h+
switch with species=
jflag= 16 csp= -7.2
data file master species= ag+
switch with species=
jflag= 1 csp= 1.0e-15
data file master species= am+++
switch with species=
jflag= 1 csp= 1.0e-15
data file master species= al+++
switch with species=
jflag= 1 csp= 1.0e-15
data file master species= b(oh)3
switch with species=
jflag= 1 csp= 1.0e-15
data file master species= ba++
switch with species=
jflag= 1 csp= 1.0e-15
data file master species= ca++
switch with species=
jflag= 1 csp= 1.0e-15
data file master species= cr+++
switch with species=
jflag= 1 csp= 1.0e-15
data file master species= cs+
switch with species=
jflag= 1 csp= 1.0e-15
data file master species= fe+++
switch with species=
jflag=19 csp= 1.0e-15
uphas1=hematite

```

```
data file master species= fe++
  switch with species=
  jflag=19  csp= 1.0e-15
  uphas1=magnetite
data file master species= li+
  switch with species=
  jflag= 1  csp= 1.0e-15
data file master species= mn++
  switch with species=
  jflag= 1  csp= 1.0e-15
data file master species= na+
  switch with species=
  jflag= 1  csp= 1.0e-15
data file master species= ni++
  switch with species=
  jflag= 1  csp= 1.0e-15
data file master species= hpo4--
  switch with species=
  jflag= 1  csp= 1.0e-15
data file master species= puo2++
  switch with species=
  jflag= 1  csp= 1.0e-15
data file master species= rb+
  switch with species=
  jflag= 1  csp= 1.0e-15
data file master species= ru+++
  switch with species=
  jflag= 1  csp= 1.0e-15
data file master species= seo3--
  switch with species=
  jflag= 1  csp= 1.0e-15
data file master species= sio2(aq)
  switch with species=
  jflag= 1  csp= 1.0e-15
data file master species= sn++++
  switch with species=
  jflag= 1  csp= 1.0e-15
data file master species= sr++
  switch with species=
  jflag= 1  csp= 1.0e-15
data file master species= zn++
  switch with species=
  jflag= 1  csp= 1.0e-15
endit.
```

Table B.2. Example Input File for the EQ6 Code

input file name= p0798.eq6.inp revised=08-JAN-1992 revisor=bpm

This run will calculate the simultaneous reeaction of P0798 glass and iron in deionized water.

endit.

```

nmodl1= 2          nmodl2= 0
tempc0= 30.        jtemp= 0
  tk1= 0.          tk2= 0.          tk3= 0.
zistrt= 0.0        zimax= 0.001
tstrt= 0.          timemx= 0.
kstpmx= 600        cplim= 0.
dzipr= 1.e+38      dzprlg= 0.2      ksppmx= 10000
dzplot= 1.e+38     dzpllg= 10000.    ksplmx= 10000
ifile= 60
iopt1-10= 0 0 0 0 0 0 0 0 0 0 0
  11-20= 0 0
ioprl-10= 0 0 0 0 0 0 0 0 0 0 0
  11-20= 0 0
iodbl-10= 0 0 0 0 0 0 0 0 0 0 0
  11-20= 0 0 0
* nxopt = number of subset selection options for suppressing minerals.
* nxopex = number of exceptions.
  nxopt= 0
* nffg = number of gas fugacities to be fixed
  nffg= 0
*   uffg= o2(g)          moffg= 0.01          xlkffg= -40.0
* nrct = number of reactants
  nrct= 2
* -----
reactant= p0798 glass
  jcode= 2          jreac= 0
  morr= 0.5        modr= 0.
  vreac= 23.78
ag      1.21E-04
am      2.64E-05
al      6.86E-02
b       2.85E-01
ba      2.24E-03
ca      3.74E-02
cr      9.21E-04
cs      3.72E-03
fe      1.79E-02
li      1.41E-01
mn      2.98E-03
na      2.26E-01
ni      2.15E-03
p       2.96E-03
pu      1.00E-05
ru      3.89e-03
se      1.26E-04
si      5.43E-01
sn      9.29E-05
sr      2.03E-03
zn      2.58E-02
o       1.94E+00
endit.

```

```

      nsk= 0          sk= 100.          fk= 0.
      nrk= 1          nrpk= 0           rk3= 0.
      rk1= 1.0        rk2= 0.          rk3= 0.
*-----
reactant= fe metal
jcode= 2          jreac= 0
morr= 0.5        modr= 0.
vreac= 7.11
fe 1.0
endit.
      nsk= 0          sk= 100.          fk= 0.
      nrk= 1          nrpk= 0           rk3= 0.
      rk1= 0.1        rk2= 0.          rk3= 0.
*-----
dlzidp= 0.10000E+39
tolbt= 1.00000E-10   told1= 1.00000E-10   tolx= 1.00000E-08
tolsat= 5.00000E-03  tolst= 1.00000E-02
screw1= 1.00000E-04  screw2= 0.00000E+00   screw3= 1.00000E-04
screw4= 1.00000E-04  screw5= 4.00000E+00   screw6= 4.00000E+00
zklogu= -6.00000E+00 zklog1= 2.00000E+00   zkfac= 9.80000E-01
dlzmx1= 1.00000E-09  dlzmx2= 1.00000E+38  nordlm= 6
itermx= 30          ntrymx= 25
npplmx= 8          nsslmx= 3          ioscan= 0
*-----
* pickup file written by eq3nr.3245R111

```

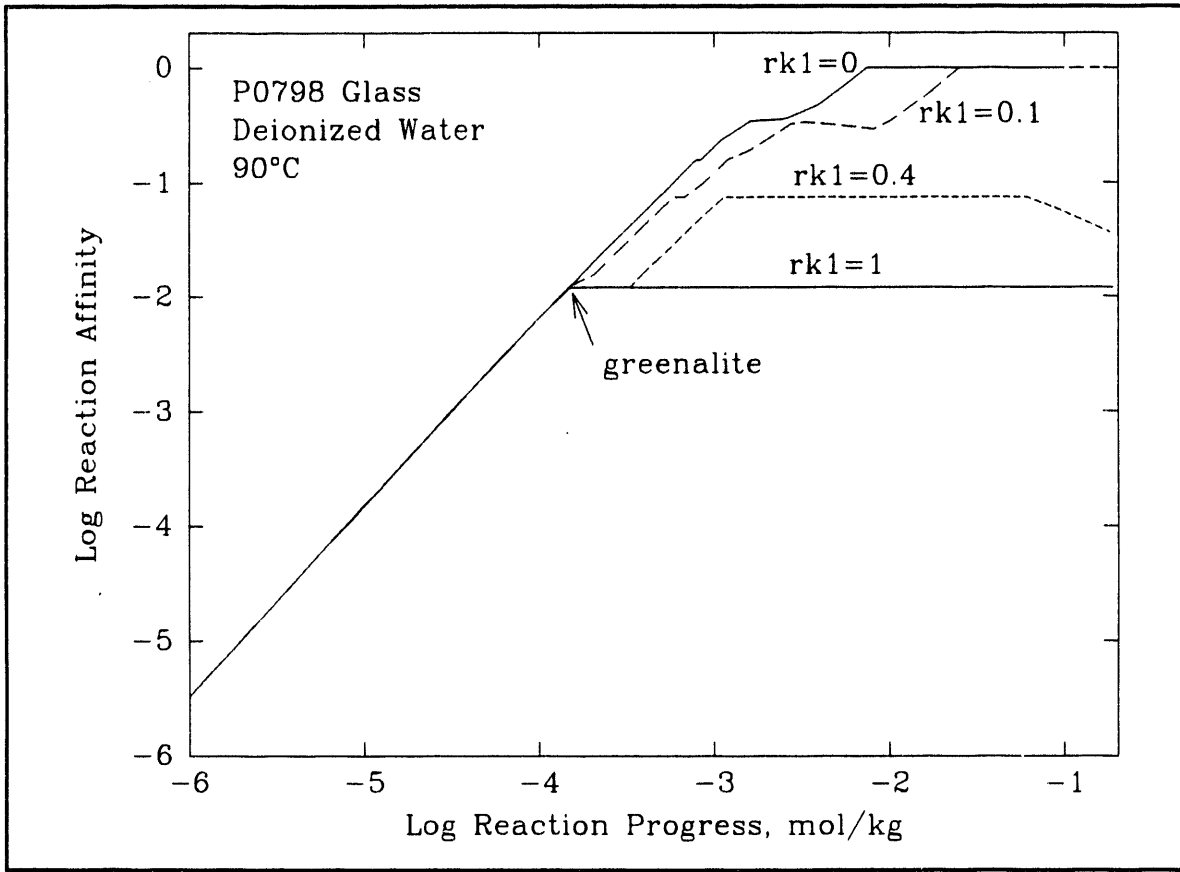


Figure B.1. Effect of Iron on the Reaction Affinity of P0798 Glass. The rk_1 values are the ratio ω/ξ as defined in Equation (54) of the main text.

Appendix C

Input and Support Code Data Files

Appendix C

Input and Support Code Data Files

AREST utilizes detailed analyses done externally, which allows a great deal of information to be used while maintaining enough efficiency in AREST to do repeated sampling and simulations. This appendix describes the actual data files that are used by AREST. The detailed analyses done for AREST are all lumped under the heading of "support codes". A brief description of the support codes utilized by AREST is contained in Section 6.0, of this document. This appendix also contains a listing of the input data file.

C.1 Input Data File

AREST is divided into three components: 1) input manager, 2) computational model, and 3) plot manager. This document describes only the computational modeling done in AREST. The input to the computational model (denoted as AREST from now on) is through a data file. This data file can either be created by hand (by modifying an existing data file) or is created by the input manager. A sample input file is shown in Table C.1. The input parameters are described in the table (file) using in-line comments (comments begin with !). The input parameters are read by sections or blocks, beginning with "#BLOCK" and ending with "#ENDBLOCK". Support code data files are read into AREST using the "#INCLUDE *filename*" statement.

C.2 Support Code Data

Support code data is either created externally and read directly into AREST or is created externally and used to guide analysis or input by hand into the input data file for AREST. The support code modeling that is read directly into AREST and discussed in this appendix includes:

- time-temperature distributions,
 - a. average container temperature
 - b. minimum repository temperature
 - c. heat loading
- groundwater composition and solubilities, and
- glass dissolution model support data,
 - a. concentrations
 - b. affinities

C.2.1 Time-Temperature Distributions

The support code TEMPEST or HEATING6 is used to create time-temperature distributions that are used by AREST for simulating temperature profiles. Temperatures are read from two different files: 1) a time-temperature distribution for a repository average temperature (Table C.2) and 2) a time-temperature distribution for a reference container temperature (Table C.3). Both of these files are created directly from the support code modeling using HEATING6.

A heat loading cumulative distribution is also needed when modeling time-temperatures in AREST. The heat loading is used to generate an initial temperature. An example of a cumulative distribution for heat loading is shown in Table C.4. This table must be created external to the support code modeling using some type of text editor. The format of the file is very important. The data must be included between the "#BLOCK heatload" and "#ENDBLOCK heatload" statements. However, the data is read using free format, with comments beginning with "!".

C.2.2 Groundwater Composition and Solubility

Table C.5, illustrates a groundwater composition data file output from EQ3/6. The table shows only a partial file from a given analysis. This file can be read directly into AREST as created by EQ3/6, and can contain any number of temperatures.

As described in the main body of text for this document, Section 7.2, solubilities can be input into AREST either as a single value (Table C.1) or as a temperature dependent value. To input a solubility as a temperature dependent value, the user must create a data file similar to the one shown in Table C.6. The data was calculated using EQ3/6 and entered using a text editor. Currently there does not exist a direct link between EQ3/6 and AREST for inputting time dependent solubilities.

This file contains the elements for which time dependent solubilities are available. Shared solubilities for each nuclide of an element are calculated using mass fractions if the shared solubility option is selected in the input file. If the shared solubility option is not selected, then each nuclide will be assigned the elemental solubility. Linear interpolation is used to estimate solubilities between temperature steps, without extrapolation.

If the user does not want to simulate solubility as a function of time/temperature, or is using some other surface concentration method (e.g., glass dissolution model or the waste alteration transport model), then the solubility file will not contain any elements. An example of the file for this type of modeling is shown in Table C.7. The file, however, must exist, since the input routine reads the file name from the input data file and then reads the file.

C.2.3 Glass Dissolution Model Support Data

The glass dissolution model, implemented in AREST, utilizes data calculated from EQ3/6 (refer to Appendix B for input to EQ3/6). Two data files are read into AREST when using the glass dissolution model. The first file contains the elemental concentrations in the void volume as a

function of reaction progress (z_i), iron content ($rk1$), and temperature. This file is illustrated with a simplified example shown in Table C.8. EQ3/6 is run separately for each temperature and thus creates a separate file for each temperature (e.g., conc50.arest and conc70.arest). These files are merged together to create the file that is read by AREST as is shown in Table C.8.

The second data file that is read by AREST when using the glass dissolution model contains the affinity values for selected mineral phases. This file is illustrated again in a simplified example shown in Table C.9. The affinities are calculated as a function of reaction progress (z_i) and temperature, and stored in separate files for each temperature. The files are then combined to form a single file containing the affinities, similar to what was done with the concentration files. The resulting files from EQ3/6 may contain several hundred mineral phases, all a function of reaction progress and temperature. Thus, a pre-processor was created to read the combined affinity files, select a mineral phase specified by the user, and write a single file containing only one mineral phase, this resultant file is shown in Table C.9.

Table C.1. Sample Input Data File for AREST

```
! AREST-PNC Data Input File
! ID      :
! Date   : Wed Apr 09 13:16:50 1992

#BLOCK Simulation_Control
  0 ! Type of sensitivity analysis
    !      0 = None
    !      1 = Base-alternate
    !      2 = Full factorial
  1 ! No. of sensitivity analysis cases
  1 ! Samples per distribution
  0 ! Seed for random number generation
  1 ! Total simulations
#ENDBLOCK Simulation_Control

! Run identification
Base Case Analysis for TSPA! run title

#BLOCK time-temp/heat
  #INCLUDE support/tuff_ref_temp.dat! reference temp file
  #INCLUDE support/tuff_min_temp.dat! min temp file
  #INCLUDE support/tuff_hl.dat! heatload file

  95      ! resaturation temperature
  1.1    ! heat load conversion
#ENDBLOCK time-temp/heat

#BLOCK solubility
  #INCLUDE support/tuff_solubility.dat! solubility file
#ENDBLOCK solubility

#BLOCK groundwater
  #INCLUDE support/tuff_envsol.dat! groundwater file
#ENDBLOCK groundwater

#BLOCK waste_package_design
  26      ! cylindrical waste radius
  441    ! cylindrical waste length
  32.5   ! cylindrical waste form radius
  454    ! cylindrical waste form length
  5      ! waste container thickness
  3      ! backfill thickness
  0      ! emplacement orientation
    !      0 --> vertical
    !      1 --> horizontal
  460    ! container spacing
#ENDBLOCK waste_package_design

#BLOCK containment
  2000   ! time of failure (yrs)
  0      ! prefailure probability
  0      ! initial prefailures
#ENDBLOCK containment

! Release control
-1      ! release control
```

Table C.1. (contd)

```

#BLOCK release
5      ! matrix release model
      !   2 --> PDS release model (wet-continuous)
      !   4 --> PDR release model (wet-continuous)
      !   5 --> PCS release model (wet-drip)
      !   6 --> PCR release model (wet-drip)
      !   7 --> FCS release model (wet-continuous)
      !   8 --> PCS release model (wet-continuous)
      !  10 --> numerical release model (STRENG)
False ! congruent release
1     ! release fractional distance
0.001 ! packing tortuosity
1     ! host rock tortuosity
2.23 ! packing density (g/m^3)
2.23 ! host rock density (g/m^3)
73   ! percentage of pores filled
1     ! glass cracking factor
2.1e+06 ! wasteform mass (g)
1.5   ! waste void width (cm)
0.6   ! waste void volume factor
False ! precipitation
False ! solubility limited
True  ! shared solubility
False ! Using Glass Dissolution Model (McGrail)?
1     ! Flag for calculating release rate or concentration
      ! 0 --> Concentration
      ! 1 --> Release rate

#BLOCK release_model_parameters

#BLOCK solubility_model
0.24 ! packing porosity
0.24 ! host rock porosity
#ENDBLOCK solubility_model

#BLOCK solubility_wet-drip_model
0.01 ! pore water flow rate (mm/yr)
#ENDBLOCK solubility_wet-drip_model

#BLOCK alteration_model
0.24 ! packing porosity
0.24 ! host rock porosity
0.755 ! reaction rate (g/m^2/d)
#ENDBLOCK alteration_model

#BLOCK alteration_wet-drip_model
0.01 ! pore water flow rate (mm/yr)
0.755 ! reaction rate (g/m^2/d)
#ENDBLOCK alteration_wet-drip_model

#BLOCK fracture_model
0.1 ! fracture thickness (cm)
250 ! fracture spacing (cm)
0.01 ! pore water flow rate (m/yr)
0.24 ! packing porosity
0.24 ! host rock porosity
#ENDBLOCK fracture_model

```

Table C.1. (contd)

```

#BLOCK convection_model
  0.01 ! pore water flow rate (m/yr)
  0.24 ! packing porosity
  0.24 ! host rock porosity
#ENDBLOCK convection_model

#BLOCK streng_model
  1 ! surface concentration flag
    !0 --> STRENG value for Csat
    ! 1 --> AREST time dependent Csat
  0.01 ! darcy flow(m/yr)
  0.24 ! packing porosity
  2 ! host rock boundary condition
    !1 --> zero concentration (swept away)
    !2 --> mixing tank
  16 ! No. of 1-D nodes in the backfill
  4 ! solution method
    !1 --> Full Discretization Method (FDM)
    !2 --> Psuedo Equilibrium Method (PEM)
    !3 --> Switching Method (FDM to PEM)
    !4 --> Fast PEM Method
  1.0e4 ! glass dissolution period (yrs)
#ENDBLOCK streng_model

#BLOCK glass_dissolution_model
  0.007 ! dissolution control volume (m^3)
  0.05 ! liquid phase volume fraction
  0.0 ! container corrosion rate (g/m^2/d)
  1 ! iron overpack crack factor
  7.8E+06! iron overpack density (g/m^3)
  0.034271! iron mass fraction
  0.293995! silica mass fraction
  64.6 ! Glass molecular weight (g-glass/mol)
  5 ! corrosion allowance (cm)
  3.25e+8! residual rate of glass dissolution (g/m^2/d)
  8.0e4 ! Activation energy (J/mol)
  0.22 ! Exponent of hydrogen ion activity
  2.32e+9! Forward rate constant (g/m^2/d)
support/affinity.dat ! affinity data file
support/conc.dat! concentration data file
chalcedony ! mineral phase
#ENDBLOCK glass_dissolution_model

#ENDBLOCK release_model_parameters

#ENDBLOCK release

#BLOCK precipitation
  1 ! precipitation fractional distance
  1 ! precipitation fractional concentration
#ENDBLOCK precipitation

#BLOCK misc_control
  False ! vector approach
  2 ! Input inventory units (1 --> g/yr, 2 --> Ci/yr)
#ENDBLOCK misc_control

#BLOCK radionuclides

```

Table C.1. (contd)

```
#BLOCK nuclide_name
U-238 ! nuclide name
U-234 ! nuclide name
Am-241 ! nuclide name
Np-237 ! nuclide name
Am-243 ! nuclide name
Pu-239 ! nuclide name
C-14 ! nuclide name
Se-79 ! nuclide name
Tc-99 ! nuclide name
Sn-126 ! nuclide name
I-129 ! nuclide name
Cs-135 ! nuclide name
#ENDBLOCK nuclide_name

#BLOCK daughter_product
U-234 ! daughter product
none ! daughter product
Np-237 ! daughter product
none ! daughter product
Pu-239 ! daughter product
none ! daughter product
#ENDBLOCK daughter_product

#BLOCK halflife
4.47E+9 ! halflife
2.45E+5 ! halflife
432 ! halflife
2.14E+6 ! halflife
7380 ! halflife
2.41E+4 ! halflife yrs
5.73E+3 ! halflife
2.11E+5 ! halflife
2.11E+5 ! halflife
1.57E+7 ! halflife
1.57E+7 ! halflife
2.3E+06 ! halflife
#ENDBLOCK halflife

#BLOCK inventory
0.63 ! inventory
4.97 ! inventory
8.09e3 ! inventory
0.859 ! inventory
48.6 ! inventory
665 ! inventory
3.29 ! inventoryg/pack
0.952 ! inventory
29.9 ! inventory
1.77 ! inventory
7.28e-2 ! inventory
0.993 ! inventory
#ENDBLOCK inventory
```

Table C.1. (contd)

```

#BLOCK solubility
  8.57E+1 ! solubility
  8.57E+1 ! solubility
  4.62E-3 ! solubility
  9.48E-1 ! solubility
  4.62E-3 ! solubility
  4.54E-6 ! solubility
  1.0     ! solubilityg/m^3
  1.0     ! solubility
  1.0     ! solubility
  1.0     ! solubility
  1.0     ! solubility
  1.0     ! solubility
#ENDBLOCK solubility

#BLOCK kd1
  2.5     ! kd1
  2.5     ! kd1
  100    ! kd1
  2.0     ! kd1
  100    ! kd1
  100    ! kd1
  0.0     ! kd1ml/g
  2.5     ! kd1
  1.0     ! kd1
  100    ! kd1
  0.0     ! kd1
  50     ! kd1
#ENDBLOCK kd1

#BLOCK kd2
  2.5     ! kd2
  2.5     ! kd2
  100    ! kd2
  2.0     ! kd2
  100    ! kd2
  100    ! kd2ml/g
  0.0     ! kd2
  2.5     ! kd2
  1.0     ! kd2
  100    ! kd2
  0.0     ! kd2
  50     ! kd2
#ENDBLOCK kd2

#BLOCK diffusion
  1.16E-05! diffusioncm^2/s
  1.16E-05! diffusion
  1.16E-05! diffusion
  1.16E-05! diffusion
  1.16E-05! diffusion
  1.16E-05! diffusion
#ENDBLOCK diffusion

```

Table C.1. (contd)

```
#BLOCK matrix_percentage
100.0
100.0
100.0
100.0
100.0
100.0
100.0
65.0
98.0
98.0
98.0
98.0
98.0
#ENDBLOCK matrix_percentage

#BLOCK gap_percentage
0.0
0.0
0.0
0.0
0.0
0.0
1.0
2.0
2.0
2.0
2.0
2.0
#ENDBLOCK gap_percentage

#BLOCK clad_percentage
0.0
0.0
0.0
0.0
0.0
0.0
32.0
0.0
0.0
0.0
0.0
#ENDBLOCK clad_percentage

#BLOCK crud_percentage
0.0
0.0
0.0
0.0
0.0
0.0
2.0
0.0
0.0
0.0
0.0
0.0
#ENDBLOCK crud_percentage
```

Table C.1. (contd)

```
#ENDBLOCK radionuclides  
#BLOCK overall_control  
35000 ! repository waste packages  
#ENDBLOCK overall_control
```

Table C.2. Example of a Repository Average Temperature Distribution File

! Time-temperature data for TUFF
! Waste Package Scale

```
#BLOCK timetemp_min
! TIME          REF TEMP
! (yrs)         (deg C)
! -----
0.005          179.99
0.27           179.99
1              216.67
5              248.01
10             249.04
20             242.74
30             233.21
40             224.02
50             213.50
70             197.39
100            183.03
200            157.00
300            143.00
400            132.00
500            126.00
1000           110.00
2000           90.00
6000           58.00
10000          47.00
100000         47.00
#ENDBLOCK timetemp_min
```

Table C.3. Example of a Reference Container Temperature Distribution File

```
! Time-temperature data for TUFF
!   Repository Scale

#BLOCK timetemp_ref
! TIME           MIN TEMP
! (yrs)          (deg C)
! -----
0.005           29.00
0.27            39.79
1               50.14
5               73.27
10              86.74
20              101.32
30              109.13
40              113.44
50              115.02
70              115.25
100             114.40
200             111.19
300             107.96
400             106.19
500             104.70
1000            98.09
2000            83.52
6000            54.23
10000           45.90
100000          45.90
#ENDBLOCK timetemp_ref
```

Table C.4. Sample Cumulative Probability Distribution for Heat Loading

! Heat Load Data for TUFF

#BLOCK heatload

! Heat Load (kW/MTU)	Cum Prob
0.2	0.0
0.5	0.11
1.0	0.57
1.2	0.82
1.5	0.96
2.0	0.99
2.5	1.0

#ENDBLOCK heatload

Table C.5. Sample Groundwater Composition Data File

TEMPERATURE	25.00	DEGREES CELSIUS
SOL. DENSITY	1.02336	G/ML
PH	7.20000	
EH	0.793	VOLTS
NA+	0.2102D-02	MOLAL CONC
CL-	0.2012D-03	MOLAL CONC
SO4--	0.1805D-03	MOLAL CONC
F-	0.1375D-03	MOLAL CONC
K+	0.1373D-03	MOLAL CONC
NO3-	0.1371D-03	MOLAL CONC
MG++	0.7998D-04	MOLAL CONC
CO3--	0.2003D-05	MOLAL CONC

TEMPERATURE	95.00	DEGREES CELSIUS
SOL. DENSITY	1.02336	G/ML
PH	7.19202	
EH	0.682	VOLTS
NA+	0.2094D-02	MOLAL CONC
CL-	0.2012D-03	MOLAL CONC
SO4--	0.1664D-03	MOLAL CONC
NO3-	0.1371D-03	MOLAL CONC
K+	0.1369D-03	MOLAL CONC
F-	0.1350D-03	MOLAL CONC
MG++	0.7016D-04	MOLAL CONC
CO3--	0.2796D-05	MOLAL CONC

Table C.6. Sample Temperature Dependent Solubility Data File

```
! Solubility data; data for TUFF
#BLOCK solubility
!           TEMP           Csat
! ELEMENT  (deg C)      (g/m**3)
! -----
!           U           100.0      4.52e-3
!           U           44.0       8.57e+1
!           Np          100.0      7.58e-2
!           Np          44.0       9.48e-1
!           Pu          100.0      1.00e-7
!           Pu          44.0       4.54e-6
!           Am          100.0      1.51e-3
!           Am          44.0       4.62e-3
#ENDBLOCK solubility
```

Table C.7. Sample File when NOT Modeling Temperature Dependent Solubilities

```
! Solubility data; Use input table from main data file
#BLOCK solubility
!           TEMP           Csat
! ELEMENT  (deg C)      (g/m**3)
! -----
#ENDBLOCK solubility
```

Table C.8. Sample Concentration Data File Used With the Glass Dissolution Model

```

! SRL-202 Glass and J-13 Groundwater
! No. of glass dissolution tables
  2

! Temperature, rk1
50,  0

! Rows, columns
9,   7

# BLOCK gd_headings
zi
pH
Am
Cs
Np
Pu
U
# ENDBLOCK gd_headings

# BLOCK gd_table
0.00E+00  8.60  2.41E-10  1.33E-10  2.37E-10  2.44E-10  0.238E-09
1.00E-10  8.60  2.75E-10  7.66E-09  9.84E-10  5.83E-10  0.114E-06
1.00E-09  8.60  5.79E-10  7.54E-08  7.70E-09  3.64E-09  0.114E-05
1.00E-07  8.60  3.40E-08  7.52E-06  7.47E-07  3.39E-07  0.114E-03
1.00E-06  8.60  3.38E-07  7.52E-05  7.47E-06  6.52E-07  0.114E-02
1.00E-05  8.61  3.38E-06  7.52E-04  7.47E-05  6.53E-07  0.114E-01
1.00E-04  8.61  3.37E-05  7.52E-03  7.47E-04  6.65E-07  0.114
1.00E-03  8.68  3.37E-04  7.52E-02  7.47E-03  7.80E-07  1.14
1.00E-02  9.03  2.20E-03  7.52E-01  7.47E-02  1.84E-06  3.52
# ENDBLOCK gd_table

! Temperature, rk1
70,  0

! Rows, columns
9,   7

# BLOCK gd_headings
zi
pH
Am
Cs
Np
Pu
U
# ENDBLOCK gd_headings

# BLOCK gd_table
0.00E+00  8.70  2.41E-10  1.33E-10  2.37E-10  2.44E-10  0.238E-09
1.00E-09  8.70  5.79E-10  7.54E-08  7.70E-09  3.64E-09  0.114E-05
1.00E-08  8.70  3.62E-09  7.52E-07  7.49E-08  3.42E-08  0.114E-04
1.00E-07  8.70  3.40E-08  7.52E-06  7.47E-07  2.79E-07  0.114E-03
1.00E-06  8.70  3.38E-07  7.52E-05  7.47E-06  2.79E-07  0.114E-02
1.00E-05  8.70  3.38E-06  7.52E-04  7.47E-05  2.80E-07  0.114E-01
1.00E-04  8.71  3.37E-05  7.52E-03  7.47E-04  2.84E-07  0.114
1.00E-03  8.77  3.37E-04  7.52E-02  7.47E-03  3.29E-07  1.14
1.00E-02  9.11  1.86E-03  7.52E-01  7.47E-02  7.53E-07  3.48
# ENDBLOCK gd_table

```

Table C.9. Sample Affinity Data File Used With the Glass Dissolution Model

```

! SRL-202 Glass and J-13 Groundwater
! No. of affinity tables
  2

! Temperature
  50.0000

# BLOCK affinity_headings
zi
pH
Eh
chalcedony
# ENDBLOCK affinity_headings

# BLOCK affinity_table
0.000E+00  8.605E+00  6.624E-01  -7.705E-02
1.000E-10  8.605E+00  6.624E-01  -7.705E-02
1.000E-09  8.605E+00  6.624E-01  -7.705E-02
1.000E-07  8.605E+00  6.624E-01  -7.699E-02
1.000E-06  8.605E+00  6.624E-01  -7.646E-02
1.000E-05  8.606E+00  6.624E-01  -7.112E-02
1.000E-04  8.613E+00  6.619E-01  -2.012E-02
1.000E-03  8.681E+00  6.576E-01  0.000E+00
1.000E-02  9.033E+00  6.349E-01  6.567E-16
# ENDBLOCK affinity_table

! Temperature
  70.0000

# BLOCK affinity_table
0.000E+00  8.702E+00  6.185E-01  -4.912E-01
1.000E-09  8.702E+00  6.185E-01  -4.912E-01
1.000E-08  8.702E+00  6.185E-01  -4.912E-01
1.000E-07  8.702E+00  6.185E-01  -4.911E-01
1.000E-06  8.702E+00  6.185E-01  -4.905E-01
1.000E-05  8.703E+00  6.184E-01  -4.849E-01
1.000E-04  8.710E+00  6.180E-01  -4.313E-01
1.000E-03  8.771E+00  6.138E-01  -1.288E-01
1.000E-02  9.107E+00  5.909E-01  2.789E-15
# ENDBLOCK affinity_table

```

Distribution

No. of
Copies

No. of
Copies

OFFSITE

12 DOE/Office of Scientific and Technical
Information

C. R. Allen
Nuclear Waste Technical Review Board
1000 E. California Boulevard
Pasadena, CA 91106

A. Anderson
Argonne National Laboratory
Building 362
9700 S. Cass Avenue
Argonne, IL 60439

E. Anderson
Mountain West Research-
Southwest, Inc.
2901 N. Central Ave., #1000
Phoenix, AZ 85012-2730

R. Andrews
INTERA
2650 Park Tower Drive
Suite 800
Vienna, VA 22180

D. H. Appel
Hydrologic Investigations
Program, MS 421
U.S. Geological Survey
P.O. Box 25046
Denver, CO 80225

M. J. Apted
INTERA Sciences
3609 South Wadsworth Blvd.
5th Floor
Denver, CO 80235

L. H. Barrett (RW-1)
Acting Director
Office of Civilian Radioactive Waste
Management
U.S. Department of Energy
1000 Independence Avenue, S.W.
Washington, DC 20585

M. L. Baughman
35 Clark Road
Fiskdale, MA 01518

D. A. Bechtel, Coordinator
Nuclear Waste Division
Clark County Department of
Comprehensive Planning
301 E. Clark Ave., Suite 570
Las Vegas, NV 89101

D. A. Beck
Water Resources Division
U.S. Geological Survey
6770 S. Paradise Road
Las Vegas, NV 89119

C. G. Bell, Jr.
Professor of Civil Engineering
Civil and Mechanical Engineering
Department
University of Nevada, Las Vegas
4504 S. Maryland Parkway
Las Vegas, NV 89154

A. Benson (RW-5)
Office of External Relations
Office of Civilian Radioactive Waste
Management
U.S. Department of Energy
1000 Independence Avenue, S.W.
Washington, DC 20585

**No. of
Copies**

**No. of
Copies**

E. P. Binnall
Field Systems Group Leader
Building 50B/4235
Lawrence Berkeley Laboratory
Berkeley, CA 94720

J. A. Blink
Deputy Project Leader
Lawrence Livermore National
Laboratory
101 Convention Center Drive
Suite 820, MS 527
Las Vegas, NV 89109

S. Bradhurst
P.O. Box 1510
Reno, NV 89505

L. W. Bradshaw
Program Manager
Nye County Nuclear Waste Repository
Program
P.O. Box 1767
Tonopah, NV 89049

J. C. Bresee (RW-10)
Office of Civilian Radioactive
Waste Management
U.S. Department of Energy
1000 Independence Avenue, S.W.
Washington, DC 20585

G. D. Brewer
Nuclear Waste Technical Review Board
The Dana Building, Room 3516
University of Michigan
Ann Arbor, MI 48109-1115

S. J. Brocoum (RW-22)
Analysis and Verification Division
Office of Civilian Radioactive Waste
Management
U.S. Department of Energy
1000 Independence Avenue, S.W.
Washington, DC 20585

R. L. Bullock
Technical Project Officer for YMP
Raytheon Services Nevada
Suite P-250, MS 403
101 Convention Center Drive
Las Vegas, NV 89109

D. Campbell
Technical Project Officer for YMP
U.S. Bureau of Reclamation
Code D-3790
P.O. Box 25007
Denver, CO 80225

4 J. A. Canepa
Technical Project Officer YMP
N-5, MS J521
Los Alamos National Laboratory
P.O. Box 1663
Los Alamos, NM 87545

J. E. Cantlon, Chairman
Nuclear Waste Technical Review Board
2795 Bramble Drive
East Lansing, MI 48823

**Center for Nuclear Waste Regulatory
Analyses**
6220 Culebra Road
Drawer 28510
San Antonio, TX 78284

**No. of
Copies**

**No. of
Copies**

3 **W. L. Clarke**
Technical Project Officer for YMP
Attn: YMP/LRC
Lawrence Livermore National
Laboratory
P.O. Box 5514
Livermore, CA 94551

**B. W. Colston, President/General
Manager**
Las Vegas Branch
Raytheon Services Nevada
MS 416
P.O. Box 95487
Las Vegas, NV 89193-5487

Community Planning and Development
City of North Las Vegas
P.O. Box 4086
North Las Vegas, NV 89030

Community Development and Planning
City of Boulder
P.O. Box 61350
Boulder City, NV 89006

R. W. Craig, Chief
Nevada Operations Office
U.S. Geological Survey
101 Convention Center Drive
Suite 860, MS 509
Las Vegas, NV 89109

J. F. Devine
Assistant Director for Engineering
Geology
U.S. Geological Survey
106 National Center
12201 Sunrise Valley Drive
Reston, VA 22092

P. A. Domenico
Nuclear Waste Technical Review Board
Geology Department
Texas A & M University
College Station, TX 77843

2 **M. J. Dorsey, Librarian**
YMP Research and Study Center
Reynolds Electrical and Engineering
Co., Inc.
MS 407
P.O. Box 98521
Las Vegas, NV 89193-8521

G. L. Ducret, Associate Chief
Yucca Mountain Project Division
U.S. Geological Survey
P.O. Box 25046
421 Federal Center
Denver, CO 80225

Economic Development Department
City of Las Vegas
400 E. Stewart Avenue
Las Vegas, NV 89101

N. Z. Elkins
Deputy Technical Project Officer
Los Alamos National Laboratory
MS 527
101 Convention Center Drive, Suite 820
Las Vegas, NV 89101

D. R. Elle, Director
Environmental Protection Division
U.S. DOE Nevada Operations Office
P.O. Box 98518
Las Vegas, NV 89193-8518

Eureka County Board of Commissioners
Yucca Mountain Information Office
P.O. Box 714
Eureka, NV 89316

**No. of
Copies**

**No. of
Copies**

	<p>C. E. Ezra YMP Support Office Manager EG&G Energy Measurements, Inc. MS V-02 P.O. Box 1912 Las Vegas, NV 89125</p>		<p>D. L. Fraser Reynolds Electrical and Engineering Co., Inc. MS 555 P.O. Box 98521 Las Vegas, NV 89193-8521</p>
	<p>P. K. Fitzsimmons, Technical Advisor Office of Assistant Manager for Environmental Safety and Health U.S. DOE Nevada Operations Office P.O. Box 98518 Las Vegas, NV 89193-8518</p>	5	<p>C. P. Gertz, Project Manager Yucca Mountain Site Characterization Project Office U.S. Department of Energy P.O. Box 98608, MS 523 Las Vegas, NV 89193-8608</p>
	<p>A. L. Flint U.S. Geological Survey MS 721 P.O. Box 327 Mercury, NV 89023</p>		<p>P. A. Glancy U.S. Geological Survey Federal Building, Room 224 Carson City, NV 89701</p>
	<p>J. Fordham Water Resources Center Desert Research Institute P.O. Box 60220 Reno, NV 89506</p>		<p>T. Hay, Executive Assistant Office of the Governor State of Nevada Capitol Complex Carson City, NV 89710</p>
	<p>J. Foremaster City of Caliente Nuclear Waste Project Office P.O. Box 158 Caliente, NV 89008</p>		<p>L. R. Hayes Technical Project Officer Yucca Mountain Project Branch-MS 425 U.S. Geological Survey P.O. Box 25046 Denver, CO 80225</p>
2	<p>L. D. Foust Nevada Site Manager TRW Environmental Safety Systems 101 Convention Center Drive Suite 540, MS 423 Las Vegas, NV 89109</p>		<p>D. Hedges Quality Assurance Roy F. Weston, Inc. 4425 Spring Mountain Road, Suite 300 Las Vegas, NV 89102</p>

**No. of
Copies**

**No. of
Copies**

	<p>E. J. Helley Branch of Western Regional Geology, MS 427 U.S. Geological Survey 345 Middlefield Road Menlo Park, CA 94025</p>		<p>M. Karakouzian 1751 E. Reno, #125 Las Vegas, NV 89119</p>
	<p>J. D. Hoffman Nuclear Waste Repository Oversight Program Esmeralda County P.O. Box 490 Goldfield, NV 89013</p>		<p>W. R. Keefer U.S. Geological Survey 913 Federal Center P.O. Box 25046 Denver, CO 80225</p>
4	<p>INTERA, Inc. 101 Convention Center Drive Phase II, Suite 540 Las Vegas, NV 89193 ATTN: R. W. Nelson A. E. Van Luik H. N. Kalia E. B. Mann</p>		<p>C. Kouts (RW-4) Office of Strategic Planning and International Programs OCRWM U.S. Department of Energy 1000 Independence Avenue, S.W. Washington, DC 20585</p>
	<p>C. H. Johnson Technical Program Manager Agency for Nuclear Projects State of Nevada Evergreen Center, Suite 252 1802 N. Carson St. Carson City, NV 89710</p>		<p>J. M. LaMonaca Records Specialist U.S. Geological Survey 421 Federal Center P.O. Box 25046 Denver, CO 80225</p>
	<p>P. S. Justus NRC Site Representative 301 E. Stewart Ave., Room 203 Las Vegas, NV 89101</p>		<p>R. Lance INTERA, Inc. 6859 Austin Center Blvd. Austin, TX 78731</p>
	<p>H. N. Kalia Project Leader for ESF Test Coordination Los Alamos National Laboratory MS 527 101 Convention Center Drive, Suite 820 Las Vegas, NV 89101</p>		<p>Lander County Board of Commissioners 315 South Humboldt Street Battle Mountain, NV 89820</p>
			<p>D. Langmuir Nuclear Waste Technical Review Board 109 S. Lookout Mountain Creek Golden, CO 80401</p>

No. of Copies		No. of Copies	
3	Lawrence Berkeley National Laboratory Earth Sciences Division 1 Cyclotron Road Berkeley, CA 94720 ATTN: K. Pruess C. F. Tsang J. Wang		R. A. Milner (RW-40) Office of Storage and Transportation OCRWM U.S. Department of Energy 1000 Independence Avenue, S.W. Washington, DC 20585
5	Lawrence Livermore National Laboratory University of California P.O. Box 808 Livermore, CA 94550 ATTN: T. A. Busheck W. L. Clarke W. J. O'Connell W. Halsey L. Lewis		P. A. Niedzielski-Eichner Nye County Nuclear Waste Repository Project Office P.O. Box 221274 Chantilly, VA 22022-1274 NRC Document Control Desk Division of Waste Management Nuclear Regulatory Commission Washington, DC 20555
3	R. R. Loux, Executive Director Agency for Nuclear Projects State of Nevada Evergreen Center, Suite 252 1802 N. Carson St. Carson City, NV 89710		Nye County District Attorney P.O. Box 593 Tonopah, NV 89049
	F. Mariani White Pine County Coordinator P.O. Box 135 Ely, NV 89301		W. Offutt Nye County Manager P.O. Box 153 Tonopah, NV 89049
	J. J. McKetta, Jr. Nuclear Waste Technical Review Board Department of Chemical Engineering CPE Building Austin, TX 78712		ONWI Library Battelle Columbus Laboratory Office of Nuclear Waste Isolation 505 King Avenue Columbus, OH 43201
	B. R. Mettham Inyo County Yucca Mountain Repository Assessment Office P.O. Drawer L Independence, CA 93526		G. J. Parker (RW-332) Regulatory Policy and Requirements Branch OCRWM U.S. Department of Energy 1000 Independence Avenue, S.W. Washington, DC 20585

**No. of
Copies**

**No. of
Copies**

	<p>T. M. Pigford Department of Nuclear Engineering University of California Berkeley, CA 94720</p>		<p>D. Rhode Desert Research Institute P.O. Box 60220 Reno, NV 89506</p>
	<p>J. Pitts Lincoln County Nuclear Waste Project Office P.O. Box 90 Pioche, NV 89043</p>		<p>J. Roberts (RW-33) Director, Regulatory Compliance Division OCRWM U.S. Department of Energy 1000 Independence Avenue, S.W. Washington, DC 20585</p>
	<p>V. E. Poe Office of Nuclear Projects Mineral County P.O. Box 1600 Hawthorne, NV 89415</p>		<p>J. D. Saltzman (RW-2) Acting Deputy Director Office of Civilian Radioactive Waste Management U.S. Department of Energy 1000 Independence Avenue, S.W. Washington, DC 20585</p>
	<p>R. F. Pritchett Technical Project Officer for YMP Reynolds Electrical and Engineering Co., Inc. MS 408 P.O. Box 98521 Las Vegas, NV 89193-8521</p>		
4	<p>V. F. Reich, Librarian Nuclear Waste Technical Review Board 1100 Wilson Blvd., Suite 910 Arlington, VA 22209</p>	4	<p>Sandia National Laboratory Department 6312 Albuquerque, NM 87185 ATTN: G. E. Barr H. A. Dockery M. A. Wilson J. Gauthier</p>
	<p>L. Reiter Nuclear Waste Technical Review Board 1100 Wilson Blvd., Suite 910 Arlington, VA 22209</p>	3	<p>Sandia National Laboratory Department 6313 Albuquerque, NM 87185 ATTN: R. W. Barnard F. W. Bingham T. E. Blejwas</p>
	<p>Repository Licensing and Quality Assurance Project Directorate Division of Waste Management U.S. Nuclear Regulatory Commission Washington, DC 20555</p>		<p>Sandia National Laboratory Department 1513 Albuquerque, NM 87185 ATTN: R. R. Eaton</p>

**No. of
Copies**

**No. of
Copies**

	<p>J. H. Sass Branch of Tectonophysics U.S. Geological Survey 2255 N. Gemini Drive Flagstaff, AZ 86001</p> <p>The Honorable C. Schank Chairman Churchill County Board of Commissioners 190 W. First St. Fallon, NV 89406</p> <p>V. R. Schneider Assistant Chief Hydrologist MS 414 Office of Program Coordination and Technical Support U.S. Geological Survey 12201 Sunrise Valley Drive Reston, VA 22092</p> <p>Senior Project Manager for Yucca Mountain Repository Project Branch Division of Waste Management U.S. Nuclear Regulatory Commission Washington, DC 20555</p> <p>D. Shelor (RW-30) Office of Systems and Compliance Division OCRWM U.S. Department of Energy 1000 Independence Avenue, S.W. Washington, DC 20585</p>		<p>L. M. Smith (RW-20) Office of Geologic Disposal Office of Civilian Radioactive Waste Management U.S. Department of Energy 1000 Independence Avenue, S.W. Washington, DC 20585</p> <p>E. L. Snow, Program Manager Roy F. Weston, Inc. 955 L'Enfant Plaza, S.W. Washington, DC 20024</p> <p>2 Southwest Research Institute Center for Nuclear Waste Regulatory Analyses 622 Culebra Road San Antonio, TX 78228 ATTN: B. Sagar J. Walton</p> <p>J. S. Stuckless Geologic Division Coordinator MS 913 Yucca Mountain Project U.S. Geological Survey P.O. Box 25046 Denver, CO 80225</p> <p>A. T. Tamura Science and Technology Division Office of Scientific and Technical Information U.S. Department of Energy P.O. Box 62 Oak Ridge, TN 37831</p> <p>Technical Information Center Roy F. Weston, Inc. 955 L'Enfant Plaza, S.W. Washington, DC 20024</p>
5	<p>L. E. Shephard Technical Project Officer for YMP Sandia National Laboratories Organization 6310 P.O. Box 5800 Albuquerque, NM 87185</p>		

**No. of
Copies**

**No. of
Copies**

8 Technical Information Officer
DOE Nevada Operations Office
U.S. Department of Energy
P.O. Box 98518
Las Vegas, NV 89193-8518

C. Thistlethwaite, AICP
Associate Planner
Inyo County Planning Department
Drawer L
Independence, CA 93526

5 U.S. Department of Energy
Yucca Mountain Site
Characterization Project Office
101 Convention Center Drive
Phase II, Suite 200
P.O. Box 98608
Las Vegas, NV 89193-8608
ATTN: J. M. Boak
 J. R. Dyer
 J. J. Lorenz
 C. M. Newbury
 A. M. Simmons

7 U.S. Department of Energy
1000 Independence Avenue, S.W.
Washington, DC 20585
ATTN: S. J. Brocoum (RW-22)
 R. A. Milner (RW-332)
 G. J. Parker (RW-322)
 J. Roberts (RW-30)
 J. Roberts (RW-33)
 S. Rousso (RW-50)
 T. Wood (RW-52)

G. Van Roekel
Director of Community Development
City of Caliente
P.O. Box 158
Caliente, NV 89008

E. D. Verink
Nuclear Waste Technical Review Board
4401 N.W. 18th Place
Gainesville, FL 32605

M. D. Voegele
Technical Project Officer for YMP
SAIC, Inc.
101 Convention Center Drive
Suite 407
Las Vegas, NV 89109

D. Warner North
Nuclear Waste Technical Review Board
Decision Focus, Inc.
4984 El Camino Real
Los Altos, CA 94062

P. J. Weeden, Acting Director
Nuclear Radiation Assessment Division
U.S. Environmental Protection Agency
Environmental Monitoring Systems
Laboratory
P.O. Box 93478
Las Vegas, NV 89193-3478

C. L. West, Director
Office of External Affairs
DOE Nevada Operations Office
U.S. Department of Energy
P.O. Box 98518
Las Vegas, NV 89193-8518

R. Williams, Jr.
P.O. Box 10
Austin, NV 89310

T. Wood (RW-52)
Director, M&O Management Division
OCRWM
U.S. Department of Energy
1000 Independence Avenue, S.W.
Washington, DC 20585

**No. of
Copies**

Sherman S. C. Wu
Branch of Astrogeology
U.S. Geological Survey
2255 N. Gemini Drive
Flagstaff, AZ 86001

D. Zesiger
U.S. Geological Survey
101 Convention Center Drive
Suite 860, MS 509
Las Vegas, NV 89109

FOREIGN

Commission of the European
Communities
200 Rue de la Loi
B-1049 Brussels
BELGIUM

ONSITE

2 DOE Richland Operations Office

D. C. Langstaff K8-50
J. J. Sutey K8-50

**No. of
Copies**

34 Pacific Northwest Laboratory

M. J. Altenhofen	K7-34
I. G. Choi	K7-15
J. M. Cuta	K7-15
R. E. Einziger	P7-14
D. M. Elwood	PORTL
D. W. Engel (5)	K7-34
M. D. Erickson	K7-02
P. W. Eslinger	K6-52
G. I. Fann	K7-15
J. A. Fort	K7-15
W. J. Gray	P7-14
K. S. Lessor	K7-22
A. M. Liebetrau	K7-34
N. J. Lombardo	K7-02
B. P. McGrail	K2-38
W. E. Nichols	K6-77
E. W. Pearson	K7-15
J. S. Roberts	K7-15
F. M. Ryan	K7-70
R. E. Westerman	P8-44
R. E. Williford	K2-44
M. D. White	K7-15
P. D. Whitney	K7-34
S. B. Yabusaki	K6-77
Publishing Coordination	
Technical Report Files (5)	

DATE

FILMED

2 / 10 / 94

END

